UNIVERZITA PALACKÉHO V OLOMOUCI

Faculty of Science

Department of Physical Chemistry

PREPARATION OF SILVER PARTICLE LAYERS FOR PURPOSES OF SURFACE ENHANCED RAMAN SPECTROSCOPY

Bachelor thesis

Author: Jana Osičková
Study programme: B1407 Chemistry
Branch of study: Applied chemistry
Form of study: Full-time
Thesis advisor: doc. RNDr. Robert Prucek, Ph.D.

Olomouc 2015

Prohlášení:

Prohlašuji, že jsem tuto bakalářskou práci vypracovala samostatně. Veškeré literární prameny a informace, které byly v práci využity, jsou v seznamu použité literatury. Souhlasím s tím, že tato práce je prezenčně zpřístupněna v knihovně Katedry fyzikální chemie, Přírodovědecké fakulty, Univerzity Palackého v Olomouci.

V Olomouci dne ……..

……..

podpis

Poděkování

Ráda bych poděkovala doc. RNDr. Robertu Pruckovi, Ph.D. za vedení bakalářské práce, odbornou pomoc, trpělivost a čas, který mi věnoval jak při práci v laboratoři, tak i během konzultací. Dále bych chtěla poděkovat Mgr. Petře Bazgerové za pořízení SEM snímků substrátů pro tuto práci.

Bibliografická identifikace:

Jméno a příjmení autora:	Jana Osičková
Název práce:	Příprava substrátů pro účely povrchem zesílené Ramanovy spektroskopie na bázi vrstev stříbra
Typ práce:	Bakalářská práce
Pracoviště:	Katedra fyzikální chemie
Vedoucí práce:	Doc. RNDr. Robert Prucek, Ph.D.
Rok obhajoby práce:	2015
Abstrakt:	Cílem této bakalářské práce byla příprava substrátů pro účely povrchem zesílené Ramanovy spektroskopie na bázi stříbra. Pomocí modifikované Tollensovy metody byly vyzkoušeny jako redukční látky glukóza, maltóza, kyselina askorbová, hydroxylamin a hydrazin. Glukóza a maltóza vykazovaly nejlepší výsledky a pracovalo se s nimi dále. Pro přípravu se použily vrstvy na bázi celulózy nebo oxidu hlinitého. Připravené substráty byly dále použity pro měření adeninu jako modelového analytu při excitační vlnové délce 785 nm. Tato vlnová délka byla vybrána kvůli výbornému využití při měření biologických analytů. Adenin při koncentraci 10^{-1} mol·dm^{-3} na nezměněném substrátu byl srovnáván s adeninem o koncentraci 10^{-4} mol·dm^{-3} na stříbrném substrátu. Celulóza polyethylenimin a celulóza MN300 substráty vykazovaly dobré Ramanovo povrchové zesílení.
Klíčová slova:	stříbrné částice, povrchem zesílená Ramanova spektroskopie, substrát, adenin, Al_2O_3, celulóza
Počet stran:	43
Počet příloh:	0
Jazyk:	angličtina

Bibliographical identification:

Author's first name and surname:	Jana Osičková
Title:	Preparation of silver particle layers for the purpose of surface enhanced Raman spectroscopy
Type of thesis:	Bachelor
Department:	Department of Physical Chemistry
Supervisor:	doc. RNDr. Robert Prucek, Ph.D.
Year of presentation:	2015
Abstract:	The aim of this bachelor thesis was the synthesis of silver particle layers for the purpose of surface enhanced Raman spectroscopy. Using a modified Tollens method, glucose, maltose, ascorbic acid, hydroxylamine and hydrazine were tested as reduction reagents. Maltose and glucose had the best results and were used further on. Cellulose and aluminum oxide layers were used for the synthesis. Prepared substrates were used for measuring adenine as a model analyte at an excitation wavelength of 785 nm. This wavelength was chosen for its good potential in measurements of biological analytes. Adenine at a concentration of 10^{-1} mol·dm^{-3} on an unaltered substrate was compared to adenine at a concentration of 10^{-4} mol·dm^{-3} on a silver coated substrate. Only cellulose polyethylenimine and cellulose MN300 substrates showed good Raman surface enhancement.
Key words:	silver particles, surface enhanced Raman spectroscopy, substrates, adenine, Al_2O_3, cellulose
Number of pages:	43
Number of appendices:	0
Language:	English

CONTENTS

1. Introduction

In the past decade, there has been an extraordinary boom in nanotechnologies. It has given way to new discoveries as well as improvement in other scientific branches. Among others, it has led to advances in an analytical method called surface enhanced Raman spectroscopy.

Surface enhanced Raman scattering (SERS) was first observed in 1974[1] and was not able to fully reach its potential until recent progress in nanotechnologies. Today we can control the size and shape of nanoparticles, which enables us to produce suitable and easily reproducible substrates for surface enhanced Raman spectroscopy. This method enables detection of analytes at very low concentrations, making it a very powerful analytical tool. The practical use of SERS is already very broad, ranging from environmental analysis of polycyclic aromatic hydrocarbons, the study of pathogenic bacteria or detection of potentially dangerous substances in food, proving that this is a perspective analytical technique.[2-20]

This bachelor thesis focuses on the production of substrates for purposes of surface enhanced Raman spectroscopy. For the preparation of substrates we used cellulose and silica gel coated layers and deposited them in a solution of silver nanoparticles that were prepared using a modified Tollens method, which formed a thin top layer on the substrates. We used maltose and glucose as the most efficient reduction agents for the preparation of silver nanoparticles and examined which substrates best deposited these nanoparticles. Surface enhanced Raman scattering was then measured using a Raman spectrometer at wavelength of 785 nm. This wavelength was chosen because of its use in efficient detection of biological analytes. The highest measured signal at 734 cm^{-1} of adenine at a concentration of 10^{-1} $mol \cdot dm^{-3}$ was compared to the enhanced signal of adenine at a concentration of 10^{-4} $mol \cdot dm^{-3}$ on silver coated substrates.

2. Theoretical part

2. 1 Raman Spectroscopy

Raman spectroscopy is an analytical method which detects molecules due to inelastic scattering of light. This phenomenon was first observed in 1928 where, in the experiment, sunlight was focused onto a sample, which scattered radiation with a different frequency.[21] Next, we will explain the basic principles of Raman spectroscopy.

2. 1. 1 Theory of inelastic light scattering

When photons interact with matter, some of them are either absorbed, scattered or do not interact with the material in any way. In the case of scattering, unlike absorption, the photon doesn't have to have a matching energy to the difference between two energy levels of a molecule. The light interacts with the molecule and polarizes the cloud of electrons around the nuclei to form a very brief state called a "virtual state". It is not stable and it quickly re-radiates.

In Raman spectroscopy, a single frequency of radiation is used to excite an analyte and the radiation, which is scattered from the molecule and is different by one rotational-vibrational unit of energy, is detected. The energy changes we detect are needed to cause nuclear motion. If only electron cloud distortion is involved in scattering, the scattering will have a minute frequency change due to the small weight of electrons. This is called elastic scattering and is a dominant process. For molecules it is called Rayleigh scattering (Fig. 1).

If nuclear motion is induced during scattering, energy will be transferred either from the molecule to the photon or vice versa. This is called inelastic scattering and the energy of the scattered photon differs by one vibrational unit from the original photon. This is Raman scattering. Since nuclei are much heavier than the electrons, there is a much bigger change in energy to either lower or higher energy depending on whether the process starts with the molecule in the ground state, Stokes scattering, or from a molecule in an excited state, anti-Stokes scattering. Most of the molecules will be in its ground state, so the majority of Raman scattering will be Stokes scattering.[22]

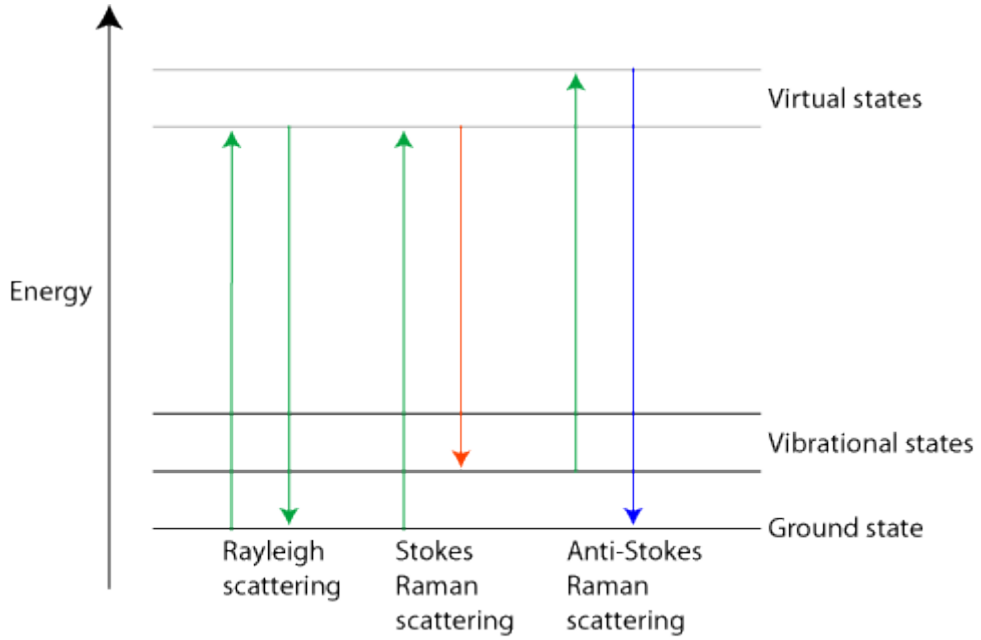

Fig. 1: Energetic interactions of light with matter – demonstration of Rayleigh, Stokes and Anti-Stokes scattering[23]

2. 2 History of surface enhanced Raman scattering

Surface enhanced Raman scattering was first observed in 1974 when pyridine was detected on a roughened silver electrode.[1] The interpretation of why this happened was not quite correct. Three years later, it was explained that the increased signal wasn't due to the larger surface area, but due to a different type of enhancement.

Until the beginning of the 21st century, this topic wasn't as popular due to lack of knowledge of nano-science and most studies were theoretical. With the rise of interest in nanoparticles, popularity of SERS rose as well. The thought that surface enhanced Raman spectroscopy could enable single molecule detection made it a very prominent topic. As we will mention later on, this is already coming close to reality. Today, this method is being applied in numerous ways, proving that it is very versatile and useful in many analyses.[24]

2. 3 Theory of Raman scattering surface enhancement

While most studies have agreed on two theories of surface enhancement, the specifics are still being looked into till this day. Before we get into the details of both theories, we can say that they both share these properties.

Electrons are situated on the surface of metal substrates. Because they are on the top, the positive charge is situated on the opposite side. When a laser interacts with these electrons, they begin to oscillate. They are called surface plasmons.

Surface plasmons have a certain variable frequency at which they absorb and scatter light efficiently. This variability is dependent on the type of metal and its surface.

Also, in order for the surface enhancement to even occur, particle size is very essential as well, with the size ranging from 5 to 100 nm. The general observation is that the size of the nanoparticles should be smaller than the wavelength of the exciting light.[25]

To point out the often used gold and silver, these particles oscillate at frequencies in the visible regions which suit the use for visible and near infrared lasers used in Raman spectroscopy. Metals both scatter and absorb allowing us to form a ratio, where scattering is more favorable. Scattering is achieved by roughening a metal surface.[24] Optical properties of specific metal colloids which present these favorable properties will be further discussed in section 2. 4. Let us take a closer look at the differences between the two theories of surface enhancement.

2. 3. 1 Electromagnetic enhancement

The principle of this theory is as follows: analyte is adsorbed onto the metal surface where interactions occur. More specifically, the molecule of an analyte is situated in a freely moving electron cloud, whose movement intensifies the polarization of the surface electrons. Electrons in the analyte interact with this electron cloud causing greater polarization.

Based on this theory, we have been able to observe some requirements needed for obtaining surface enhancement, one of which is distance of the analyte from the surface. The further a particle is from the surface, the smaller the surface enhancement.

Enhancement has been observed in bigger clusters rather than just single particles. These big SERS active clusters are called “hot spots”, proving that enhancement isn’t evenly dispersed on the surface. The reason for their higher activity is due to their shared plasmons. Each particle has a plasmon for which the resonance condition is satisfied by a small range of wavelengths, but electrons have a tendency to couple with other close particles which then share the plasmon and have a new range of wavelengths that fit its resonance condition.

When these particles touch, they also generate a large electric field which gives effective SERS. Other parameters such as particle size and shape, organization of clusters contribute to SERS enhancement as well.[22]

2. 3. 2 Chemical enhancement

The existence of chemical enhancement is to this day often debated over due to the small contribution to the overall enhancement factor and due to other chemical effects affecting SERS intensity, such as molecule adsorption or orientation.

Simply put, chemical enhancement the process of the analyte chemically bonding to the surface and electrons being transferred between the analyte and the metal surface. This is called the charge-transfer mechanism, where the modified polarizability is more resonant with the excitation than the original one. Chemical enhancement then adds up to any existing electromagnetic enhancement, although it does not contribute greatly to the overall enhancement factor. [22,24]

2. 4 Optical properties of noble metals

Metals such as silver, gold, aluminum or copper have free conduction electrons. This makes them good conductors of heat and electricity. This quality is connected with the materials optical properties. The free electrons move in a background of fixed positive ions, which on the outside appear neutral. This forms a plasma called solid-state plasma. The optical properties in the visible spectrum are caused by this plasma.[24]

Colloids interact with photons by either absorbing or scattering. Depending on the character of the colloid, one or the other effect is stronger. These effects are also dependent on the size of the particles in the colloid.

In the case of absorption, the particles absorb the energy of the photons which increases the energy of the molecules and is subsequently transformed into thermal energy. This effect is described by the Lambert-Beer Law:

$$A = -\log\frac{I}{I_0} = \varepsilon c d$$

During scattering, the absorbed energy does not cause any energy changes, but the energy is then scattered randomly into all directions without any change in wavelength. This is called elastic scattering.

Light scattering is demonstrated well with Mie vector diagrams (Fig. 2). We can see that small particles have the smallest light intensity in the 90° angle and the biggest intensity

is in the direction and in the opposite direction of the incident light. When the particles are bigger, the intensity of scattered light is weakest for angles bigger than 90°.

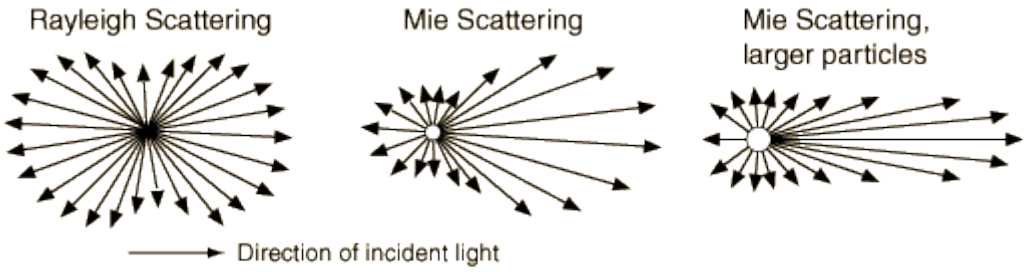

Fig. 2: Comparison of Rayleigh scattering and Mie scattering on particles of different sizes[26]

Light scattering may be explained using the following equation:

$$\left(\frac{I}{I_0}\right)_V = \frac{16\pi^4}{r^2\lambda^4} \cdot \left(-\frac{\alpha}{4\pi\varepsilon_0}\right)^2$$

But this equation can be specifically used only for small round particles (d = λ/20) which are adequately distant from each other. From this we can deduce that light scattering grows with the decreasing wavelength and with the increasing particle size.[27]

Nonetheless, particles can have many different shapes, so there is a need to calculate light scattering using other methods. For example, we can use the discrete dipole approximation (DDA), which is described by dividing a particle into an array of cubes, which have a derived polarizability from the material's dielectric constant. The reaction against an electromagnetic field is described by the dipole moment in each divided cubic part. Other methods that may be used is the modified long-wavelength approximation (MLWA) which can be applied to the dynamics of single particles but in combination with single dipole per particle approximation (SDA), we can use it for particle clusters.[28] In Fig. 3a, we can see a comparison of these three theories with extinction spectra of 30 nm round silver nanoparticles.

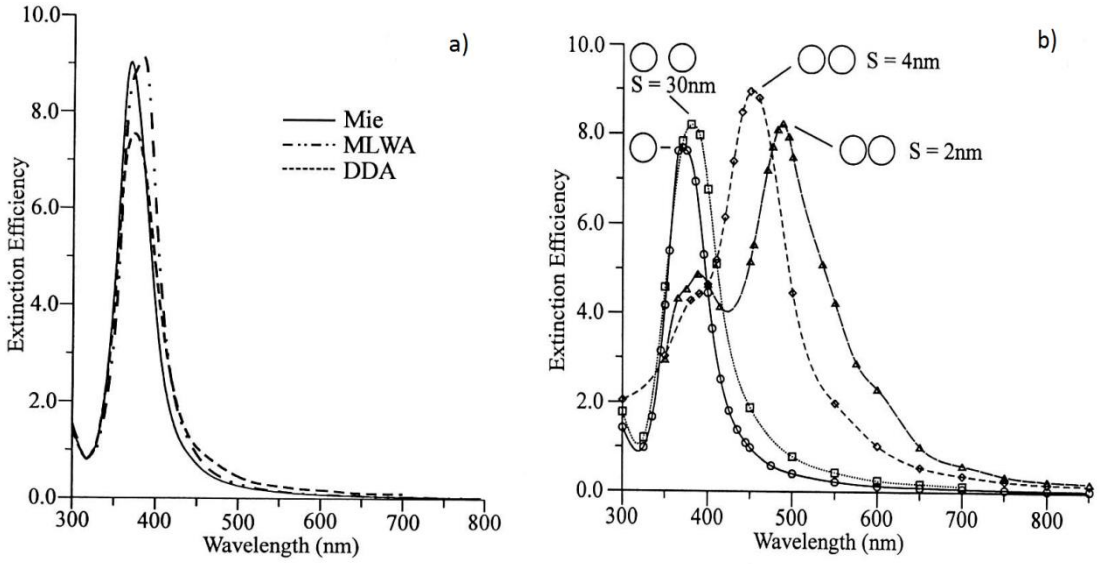

Fig. 3: a) Comparison of extinction efficiency against wavelength for 30 nm silver nanoparticles for methods Mie, MLWA and DDA, b) Comparison of extinction efficiency against wavelength for 30 nm silver nanoparticles which are separated by 30 nm, 4 nm and 2 nm[28]

Spacing between particles is also one of the variables which can alter the optical properties of a particle (Fig. 3b). Definitely worth mentioning is also how shape and size of a particle can shift the wavelength.

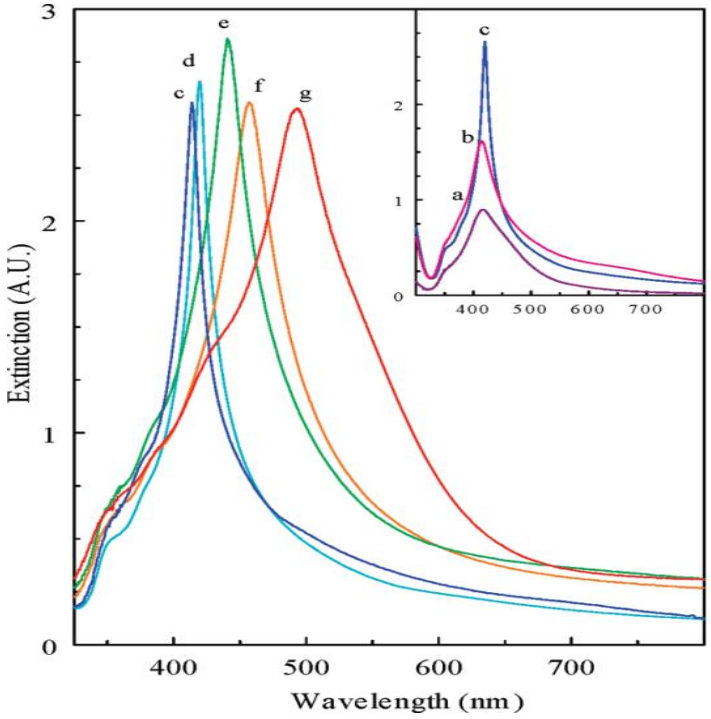

Fig. 4: Extinction spectra of silver nanoparticles at sizes a) 46 nm, b) 59 nm, c) 86 nm, d) 128 nm, e) 160 nm, f) 194 nm and g) 278 nm.[29]

In Fig. 4 we can see that with the growth of the particle size, there is a shift to longer wavelengths.[29] In Fig. 5, if we look at the spectra of silver particles, they are narrower than the spectra of gold nanoparticles, even when the shape of the two types of silver nanoparticles is different.[30]

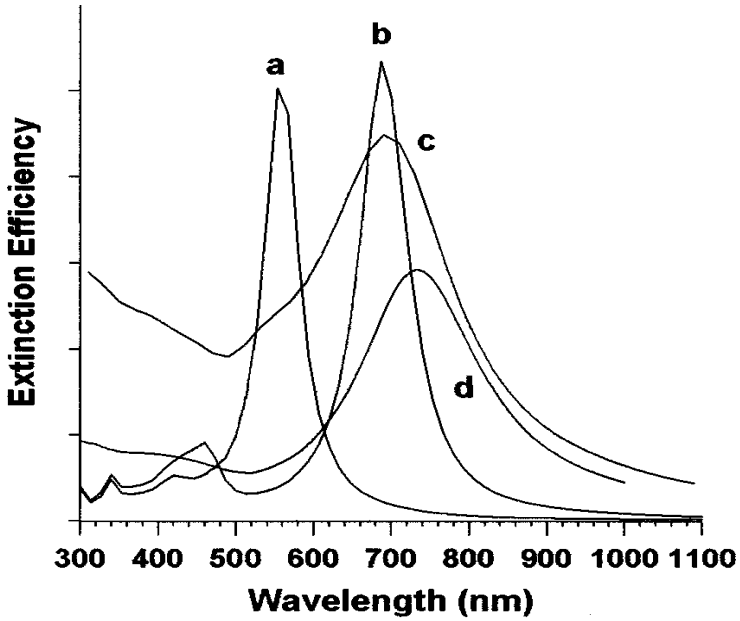

Fig. 5: Extinction spectra of a) 40 nm silver nanodisks, b) 60 nm silver triangular nanoprisms, c) 48 nm three-tip branched gold nanocrystals, d) 18 nm gold nanoshells[30]

2. 5 Preparation of SERS substrates

Ways of preparing substrates are already very diverse. All ideal substrates share properties which then give the best surface enhancement. Firstly, the substrate should have a high SERS activity due to the control of nanoparticles size and interparticle spacing. Next, the substrate should be well arranged, stable and have a long shelf life. It should also be manufactured reproducibly and reach a satisfying level of purity, so that there are no interferences while measuring weak adsorbates or unknown samples.[31]

The first SERS substrates that were used were roughened electrodes. They are not used as much these days, but we can still find more sophisticated versions of this type of substrate.

For example, silver electrode-posited screen-printed electrodes were used for qualification and quantification of polar organic pollutants. The screen printed electrode was submersed in an $AgNO_3$ solution for a specified time at specific potentials. They were then dried and used to measure different analytes.[2]

The simplest and most used method is the chemical reduction method, in which a metal salt is reduced to metal nanoparticles in aqueous or nonaqueous solution by reductants.[3] Some substances are added to the solution to prevent aggregation or oxidation of the synthesized nanoparticles or to adjust their shape or size. Many factors influence the whole process, namely type of metal salt, reductant, temperature, pH and concentrations of all the substances.

Simple round shaped nanoparticles can be altered into different shapes via the growth processes. While being vigorously stirred a solution of $HAuCl_4$, NH_2OH, $AgNO_3$ and gold seeds ended up producing thorny gold nanoparticles.[4] With any specific process, the shape of the nanoparticles can be altered.

Other methods, which are becoming very significant, are nanosphere lithography, chemical assembly method and anodic aluminum oxide template method.[31]

2. 6 Types of SERS substrates

SERS substrates are strongly wavelength dependent. Most substrates work in a limited range of wavelengths, usable mostly in visible or near-infrared excitation ($400-1000$nm). This is due to the structures made from gold or silver, most common metals used for SERS substrates and their size being smaller than the used excitation wavelength, which is typically under 100 nm. Today, we can classify SERS substrates into these groups:[24]

- metallic electrodes
- metallic particles in a colloidal solution
- planar metallic substrates

Here, we will mention some of the most interesting and the most promising SERS substrates.

There has been increased interest in molecular imprinting technique for higher selectivity and sensitivity – specifically core-shell imprinted nanoparticles. Gold nanoparticles anchored on a silica monomer template were able to selectively detect bisphenol A (BPA) in real life samples. The selectivity of this particular substrate was due to the interaction of BPA through hydrogen bonds.[5]

Spherical shaped particles as substrates are also used very often because they offer a much bigger adsorption surface. They are coated in various layers of SERS active molecules and may be composed of more than just one layer. It is quite vital to keep the layers as close together as possible.[6]

3D SERS substrates are a very interesting novelty.[7] In this specific study, ZnO nanorods covered with silver nanoparticles showed, that the structure could be perfectly engineered. It provided a much larger surface for analyte adsorption than a flat surface, the exact size of silver nanoparticles ensured the highest enhancement factor, detecting rhodamine 6G at the concentration of 10^{-12} $mol \cdot dm^{-3}$, and proved very good uniformity from measurements of 10 different points. This looks to be very promising in the future.

Another type of substrate, which is very prominent thanks to its reusability is a silver-electrode-posited screen-printed electrode.[2] They have been used for quantification and qualification of polar organic pollutants which were selectively adsorbed in just 5 minutes at a given potential. The electrodes showed great SERS activity due to its rough and porous morphology which provided large surface area and "hot-spots".

Mass fabrication of substrates is also a high priority. SERS substrates need to be produced reproducibly in larger amounts and in a simple manner. Screen printing technique may offer the solution to this problem.[8] A batch of silver coated glass substrates was fabricated with this method and it showed good enhancement factors over a longer period of time and had consistent spectra.

2. 7 Application of SERS

Over the past decade, SERS has proven to be a useful tool in many fields of analysis, whether it is health, food, military or environmental issues. We will look closer at how helpful this method is in different branches.

2. 7. 1 Organic pollutants

Due to human carelessness, our environment has been polluted by many harmful substances. Because of this, there is a need to detect these pollutants to prevent them from spreading, but also to eliminate them completely.

Bisphenol A has been used for the production of plastic products and has a risk of being released into our food and water after being discarded into the environment thus inevitably entering the food chain. We now have an ability to detect BPA with highly selective molecular imprinted polymer Au nanoparticles, which showed great results during experiments with real life samples.[5]

Among many problematic pollutants are polychlorinated biphenyls. PCBs are persistent organic pollutants, compounds that resist chemical, biological and photolytic degradation, causing accumulation in the environment and in the food chain.[32] Toxic doses of PCBs

are very low; therefore the smallest limit of detection is needed. Ag films over nanosphere substrates with self-assembled monolayer of decanethiol reached the limit of 50 $pmol \cdot dm^{-3}$. Adsorption of PCBs only took 1 minute and spectra of two close types of PCBs were distinguishable. This type of sensor was reusable, thus enabling multiple measurements on one substrate and avoiding problems with excessive waste.[9] 3D SERS substrates were also used for detection of PCBs, reaching the lowest concentration at 10^{-11} $mol \cdot dm^{-3}$.[7]

Some pollutants pose a problem in detection. Polycyclic aromatic hydrocarbons (PAHs) do not have the needed affinity to metal nanoparticles as other SERS active molecules. Functionalizing substances such as calixarenes may have solved this problem. In this study, PAHs were detected by interacting with dithiocarbamate calix(4)arene functionalized Ag nanoparticles. Main focus was on four different types of PAHs, which differed in size and thickness. Quantification of these pollutants and the specific interactions between the analytes and the substrates were studied. Therefore in this case Surface enhanced Raman spectroscopy could also be used for observing structural information of molecules.[3]

2. 7. 2 Food industry

High quality and non defective groceries have become a standard in our society. Unfortunately, our fast paced world isn't affecting our food positively. A prime example of this is antibiotics, which are given to healthy livestock that we consume. In order to avoid overuse of antibiotics, it is necessary to detect them in time before we have them served on our plate in a steak.

Restricted antibiotics were detected using silver dendrites as substrates and reached ppb levels of detection at excitation wavelength of 785 nm. This was done in a simple aqueous solution, not in a real food sample, which of course would have been preferable.[10]

Food is also often contaminated with bacteria which can cause serious diseases. *E. coli* is one of the most common bacteria which we can find in contaminated foods; therefore methods are being devised for its detection to prevent a wider spread of this bacterium. Intracellular nanosilver as a substrate was used for in vivo molecular probing and was able to differentiate individual bacteria in a mixed sample and was able to detect even single cells.[11]

In the case of food contamination, it could be taken advantage of and become a powerful means for bioterrorism. Ricin is a protein toxin which naturally occurs in castor beans. It

may be used as a potential bioterrorist weapon due to its high toxicity. In this study, ricin is separated from milk using immunomagnetic separation and then detected on a substrate of Ag dendrites. This method detected 4 μg/ml ricin in milk within 20 minutes.[12]

2. 7. 3 Bacteria discrimination

In microbiology, rapid and reagentless detection of microorganisms is a much needed characteristic for analytical methods. Time especially plays a very important role in identifying different strains of bacteria. It would quicken targeted prescription and help further advances in epidemiology. Water is a weak Raman scatterer, which is quite convenient due to most biological samples occurring in aqueous solutions. What may pose a problem in case of some biological analytes is fluorescence, which would interfere with Raman spectra.[33]

Helicobacter pylori, a bacterium which causes gastrointestinal diseases, was detected by coupling with a silver colloid solution reduced by citric acid and consequently using photo-reduction.[13]

Use of highly controlled methods to detect mix of bacteria at near-infrared excitation wavelength using nanospheres on nanocrystals prepared with a bottom-up assembly.[11] Simple methods can be also used for the detection of a mix of bacteria, specifically 7 different types of bacteria were detected by a simple silicon wafer coated with gold adhered to a glass slide.[14] Spectra of all 7 types were successfully discriminated.

Streptococcus bacteria and *Staphylococcus Aureus* cause very severe diseases that could be preventable by timely and fast detection. Thorny golden nanoparticles, or any other types of nanoparticles, were synthesized and linked to bacteria-specific antibodies in order for the bacteria to even interact with the nanoparticles.[4] This method of substrate synthesis was often used in the case of bacteria detection.[15,16] Bacteria such as *E. coli* may also be contaminants in water. Using a flow-through system on a microarray cell, contaminated water samples were measured at very low concentrations. This method is non-destructive and has very high potential of being used with real life samples.[17]

2. 7. 4 Application in medicine

Surface enhanced Raman spectroscopy is also beginning to be used in the field of medicine. With substrates being more selective, they are less prone to interferences from various environments. For example, superoxide anion radicals have been detected using Au NPs/cytochrome c as a SERS nanosensor in live liver cells.[18] Because superoxide anion radical has no SERS response, cytochrome c as a redox active protein was used for quantification. Though this was measurable at only 532 nm excitation wavelength, it reached micro molar levels of detection. The detection of bacteria, which we mentioned before in section 2. 7. 3, is also applicable in medicine, but so far it will still take a couple of years of testing in order for it to be fully usable in practice.

2. 7. 5 Detection of explosives

Detection of explosives is very important in any aspects of life which require safety. The presence of explosives is not only from the past, where some remains are left in the soil and cause contamination, but it is a risk in vulnerable areas such as airports and any other places with a high concentration of civilians.

2,4,6-Trinitrotoluene is a very common compound used for fabrication of explosives. TNT contaminates soil and water which is a major problem due to its biological persistence, toxicity and mutagenicity. Using cysteine modified gold nanoparticles, TNT was detectable within 10 minutes at a 2 $pmol \cdot dm^{-3}$ level.[19] In another study Fe_3O_4/Au/lignin coated microspheres were used to detect TNT as well using lignin thanks to its high affinity towards TNT. It was also detectable at a 2 $pmol \cdot dm^{-3}$ level.[6]

Dinitroanisole, which is a less sensitive melt-cast medium used as a replacement for TNT, was detectable in water at limits of tens of micrograms per liter using Ag nanoparticles modified by L-cysteine methyl ester hydrochloride, and was able to overcome interferences from naturally occurring ions in water.[20]

3. Experimental part

Chemicals:

For the following experiments, we used silver nitrate (Fagron), ammonium hydroxide solution (28,0 − 30,0% NH_3 basis, Sigma-Aldrich), sodium hydroxide micropearls (g.r., Lach-Ner), maltose monohydrate (≥ 99%, Sigma-Aldrich), glucose (≥ 99,5%, Sigma), ascorbic acid, hydrazine hydrate (50 − 60% N_2H_4, Sigma Aldrich), hydroxylamine hydrochlorid (99%, Sigma Aldrich), tin(II) chloride (98%, Sigma-Aldrich).

As substrates, we used sheets of silica gel, aluminium oxide, polyamide 6, cellulose MN 300, mixed cellulose MN 300 DEAE, microcrystalline cellulose and cellulose polyethylenimine (Macherey-Nagel, Germany).

Experimental equipment:

For the SERS experiments we used iRaman Plus with the 785 nm excitation laser (BWTEK Inc., USA). The laser power was 100 mW, collection time 5s and 6x accumulation. During the measurements, the laser was focused onto the center of a droplet of adenine deposited on a substrate at a distance of about 1,5 cm.

Preparation of silver coated substrates:

Firstly, we prepared two solutions for the synthesis of silver nanoparticles. The first solution was prepared by dissolving 0,24 g of silver nitrate in a 25 ml volumetric flask, then adding 0,5 ml of ammonia and filling it up with deionized water. The second solution was prepared by dissolving 0,0533 $mol \cdot dm^{-3}$ of the reduction reagent and 0,134 g of sodium hydroxide in a 25 ml volumetric flask.

As the reduction reagents, glucose, maltose, hydrazine, ascorbic acid and hydroxylamine were used. Concentration of the reagents were either kept the same or diluted twice. Selected sheets were cut up into pieces of about 5 × 1 cm and were put into Petri dishes.

The following coated sheets were used:

- polyamide 6
- silica gel
- cellulose MN 300 (on polyester sheets)
- mixed cellulose MN 300 DEAE
- microcrystalline cellulose (on plastic sheets)
- cellulose polyethylenimine
- aluminium oxide

Then 1,5 ml of the first solution with silver nitrate diluted with 1,5 ml of deionized water were put into the Petri dish and mixed. Next, 3 ml of the second solution with the reducing reagent was mixed in while moving the Petri dish in circular movement. In a few seconds, dark silver nanoparticles started forming. The Petri dish was kept in movement until the sheet was covered with nanoparticles or until the sheet had visibly changed colour. The sheet was left in the mixture for about 5 more minutes and then washed out the solution or any other undesirable clusters. Then the sheets were left to dry on air.

Activation of coated sheets with tin dichloride

Solution of Sn^{2+} ions was prepared by dissolving 1 g of dehydrate tin dichloride in 50 ml of deionized water. Then the selected sheet was submersed in 4 ml of tin dichloride for 4 minutes. Next, the sheet was taken out, washed off with deionized water and coated with silver nanoparticles according to the already mentioned synthesis.

SERS experiments

With all the prepared silver coated substrates, we proceeded to measure its surface enhanced Raman scattering. Substrates were measured on a Raman spectrometer at a wavelength of 785 nm. For the evaluation of Raman enhancement, a solution of adenine was measured at different concentrations. First the spectra of 0,1 $mol \cdot dm^{-3}$ adenine on a non-silver coated sheet were measured, and then the spectra of 0,0001 $mol \cdot dm^{-3}$ adenine on silver coated substrates were measured.

4. Results and discussion

Preparation of silver coated substrates:

Glucose and maltose proved to be the best reduction reagents. Synthesized silver nanoparticles deposited well on the surface of the sheets and they didn't aggregate into clusters. Ascorbic acid and hydrazine didn't deposit onto the surface of the sheets, instead they deposited onto the non coated side of the sheets which was undesirable. Hydroxylamine didn't deposit onto the surface at all, it formed clusters of silver nanoparticles. According to the results, we continued to work with glucose and maltose as reduction reagents.

Glucose was used at a concentration of 0,0267 $mol \cdot dm^{-3}$ because if it was kept at the original concentration, the silver nanoparticles started to make clusters. Maltose was used at both concentrations which were 0,0267 $mol \cdot dm^{-3}$ and 0,0533 $mol \cdot dm^{-3}$. During the SERS experiments, we proved that the concentration 0,0533 $mol \cdot dm^{-3}$ of maltose was the most efficient.

All of the coated sheets were prepared successfully except for polyamide 6. It floated on top of the colloid solution and therefore silver nanoparticles couldn't be deposited on its surface. The rest of the sheets were successfully prepared with maltose and glucose as reduction reagents. The substrates often changed color and gained a darker shade as we can examine on the following photos (Fig.6 − 15).

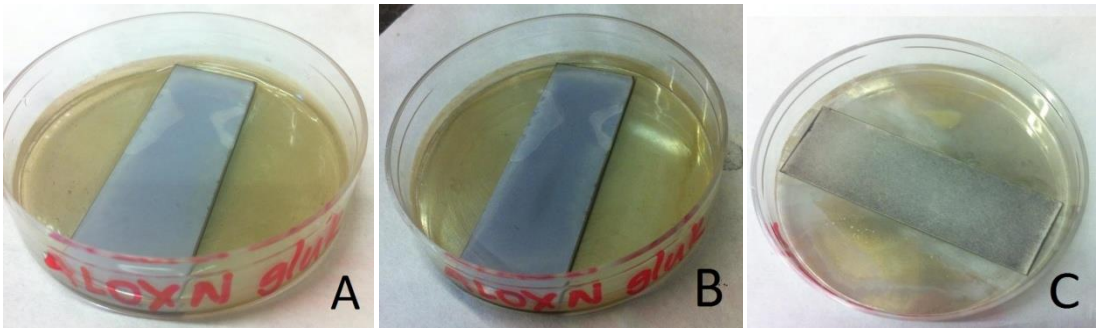

Fig. 6: Silver particle layers on aluminium oxide N substrates prepared by using glucose as a reduction reagent. Digital photo of silver particle layers: A) immediately after preparation, B) 1 week after preparation, C) 4 months after preparation

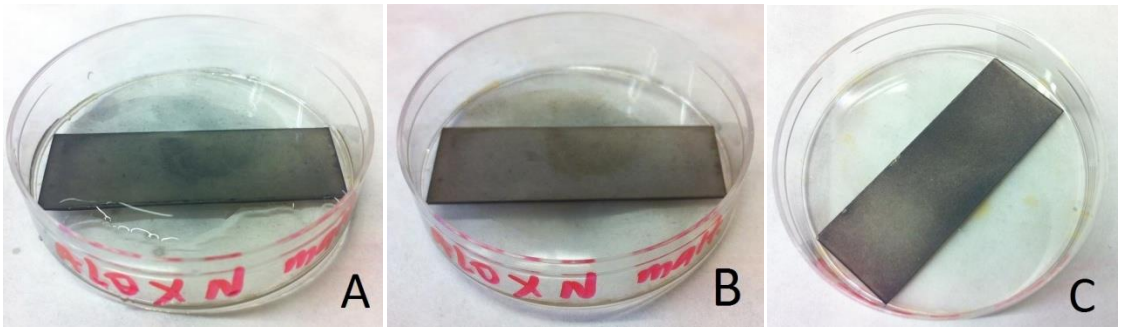

Fig. 7: Silver particle layers on aluminium oxide N substrates prepared by using maltose as a reduction reagent. Digital photo of silver particle layers: A) immediately after preparation, B) 1 week after preparation, C) 4 months after preparation

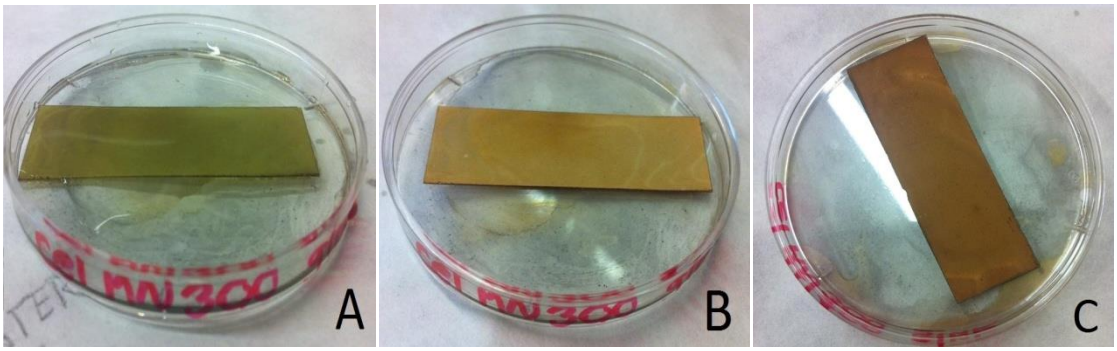

Fig. 8: Silver particle layers on cellulose MN 300 substrates prepared by using glucose as a reduction reagent. Digital photo of silver particle layers: A) immediately after preparation, B) 1 week after preparation, C) 4 months after preparation

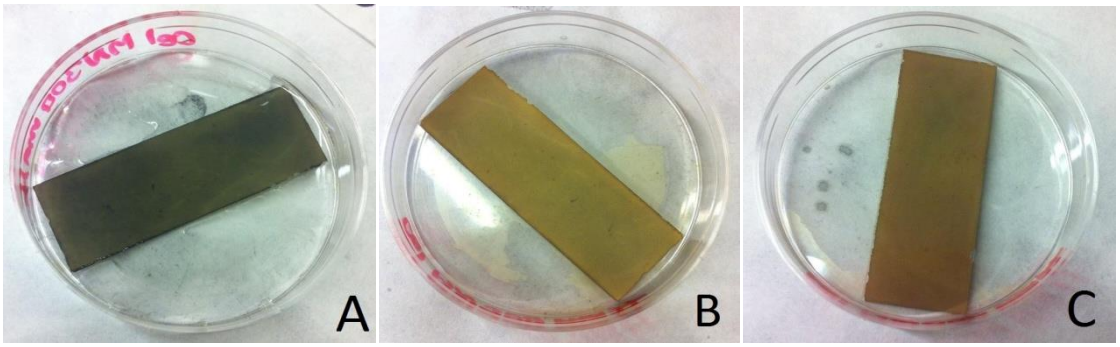

Fig. 9: Silver particle layers on cellulose MN 300 substrates prepared by using maltose as a reduction reagent. Digital photo of silver particle layers: A) immediately after preparation, B) 1 week after preparation, C) 4 months after preparation

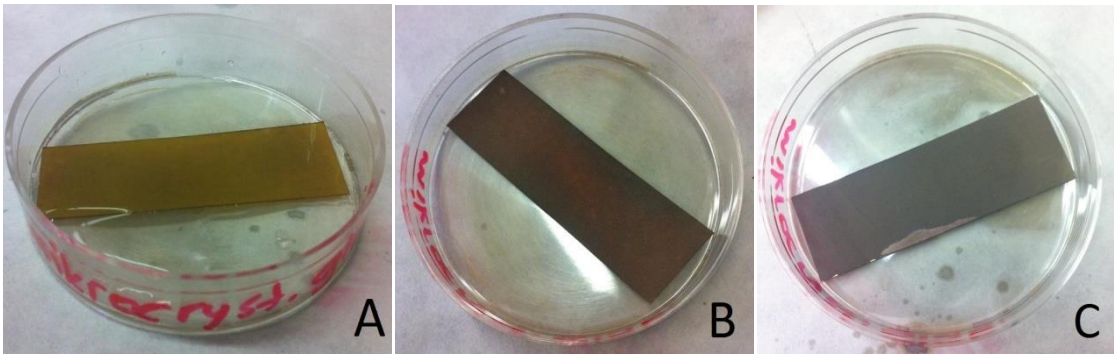

Fig. 10: Silver particle layers on microcrystalline cellulose substrates prepared by using glucose as a reduction reagent. Digital photo of silver particle layers: A) immediately after preparation, B) 1 week after preparation, C) 4 months after preparation

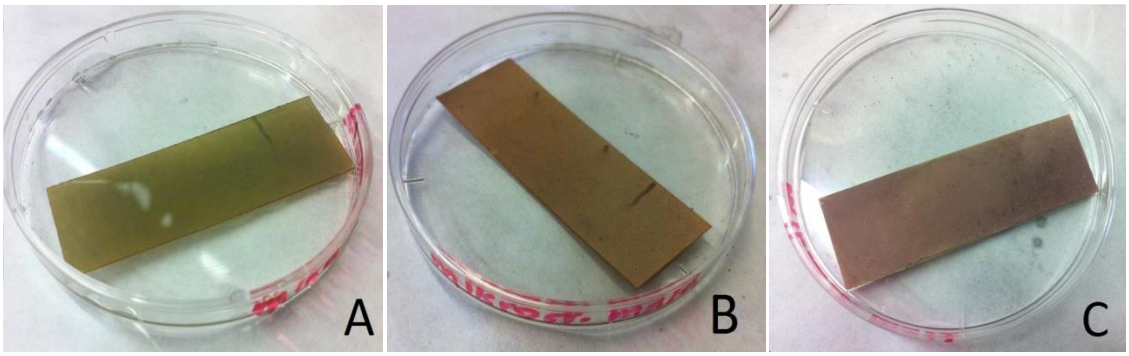

Fig. 11: Silver particle layers on microcrystalline cellulose substrates prepared by using maltose as a reduction reagent. Digital photo of silver particle layers: A) immediately after preparation, B) 1 week after preparation, C) 4 months after preparation

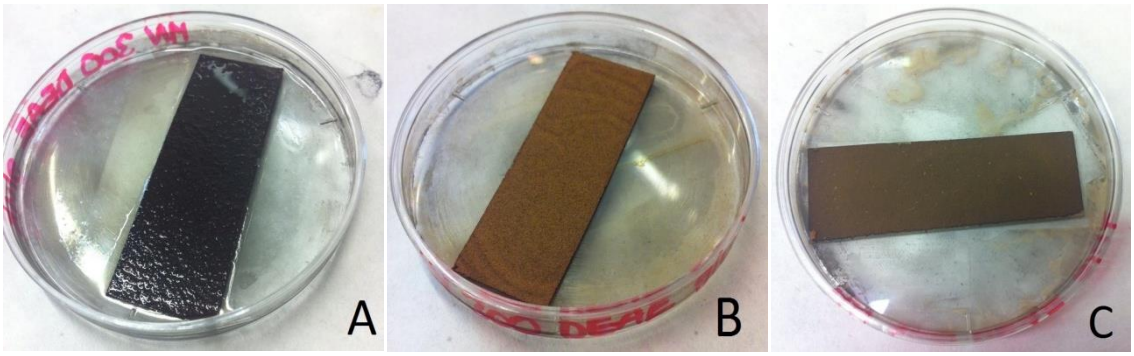

Fig. 12: Silver particle layers on mixed layer of cellulose MN 300 DEAE substrates prepared by using glucose as a reduction reagent. Digital photo of silver particle layers: A) immediately after preparation, B) 1 week after preparation, C) 4 months after preparation

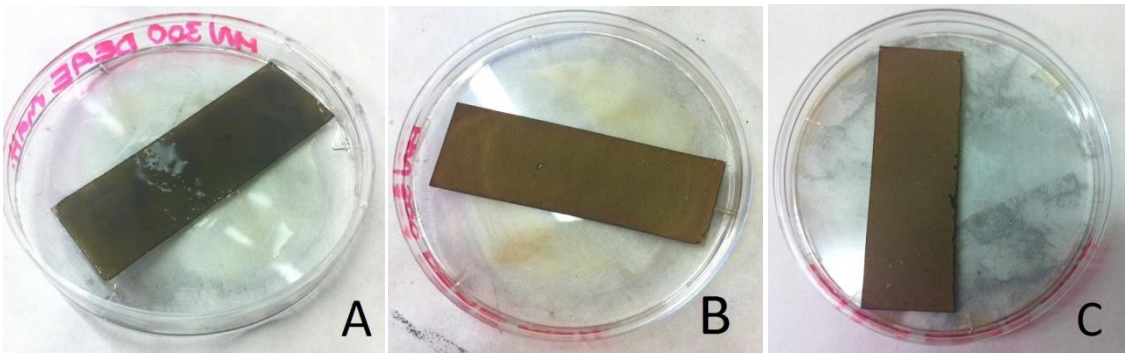

Fig. 13: Silver particle layers on mixed layer of cellulose MN 300 DEAE substrates prepared by using maltose as a reduction reagent. Digital photo of silver particle layers: A) immediately after preparation, B) 1 week after preparation, C) 4 months after preparation

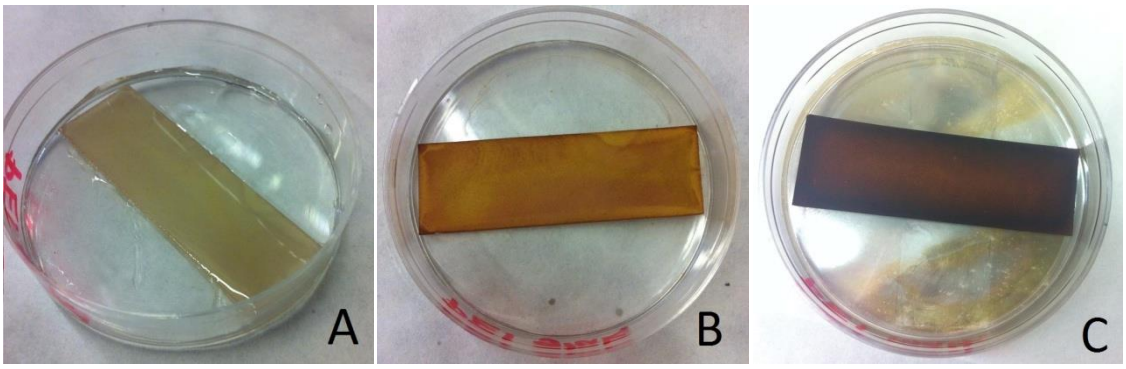

Fig. 14: Silver particle layers on cellulose polyethylenimine substrates prepared by using glucose as a reduction reagent. Digital photo of silver particle layers: A) immediately after preparation, B) 1 week after preparation, C) 4 months after preparation

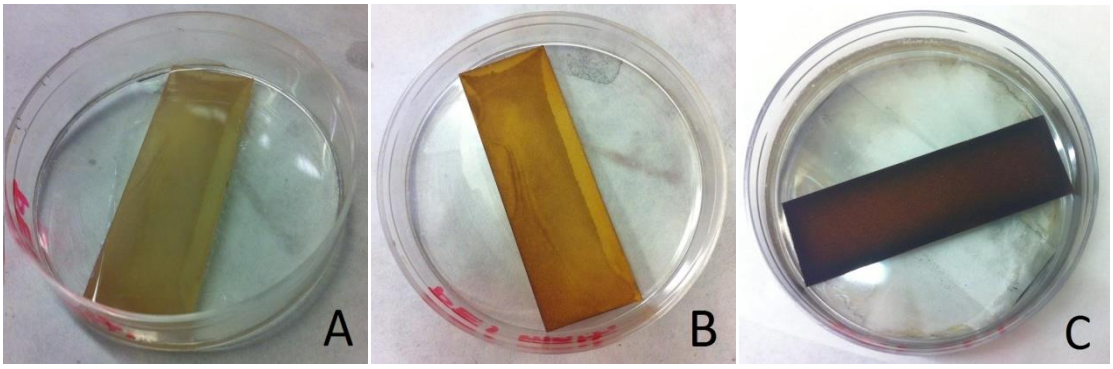

Fig. 15: Silver particle layers on cellulose polyethylenimine substrates prepared by using maltose as a reduction reagent. Digital photo of silver particle layers: A) immediately after preparation, B) 1 week after preparation, C) 4 months after preparation

We can see that over time, there was visible degradation of the substrates, probably due to the oxidization of the silver. Therefore it would be best to keep the substrates in an inert atmosphere to prolong their usability.

Activation of coated sheets with tin dichloride

The use of tin dichloride proved to be unsuccessful. After leaving coated sheets in the solution of tin dichloride, we continued to prepare silver nanoparticles, which didn't adsorb onto the surface of the sheets, but instead adsorbed onto the surface of the Petri dish. Therefore this procedure could not be used.

SERS experiments

The activity of substrates was measured on the Raman spectrometer at wavelength 785 nm and had the following results:

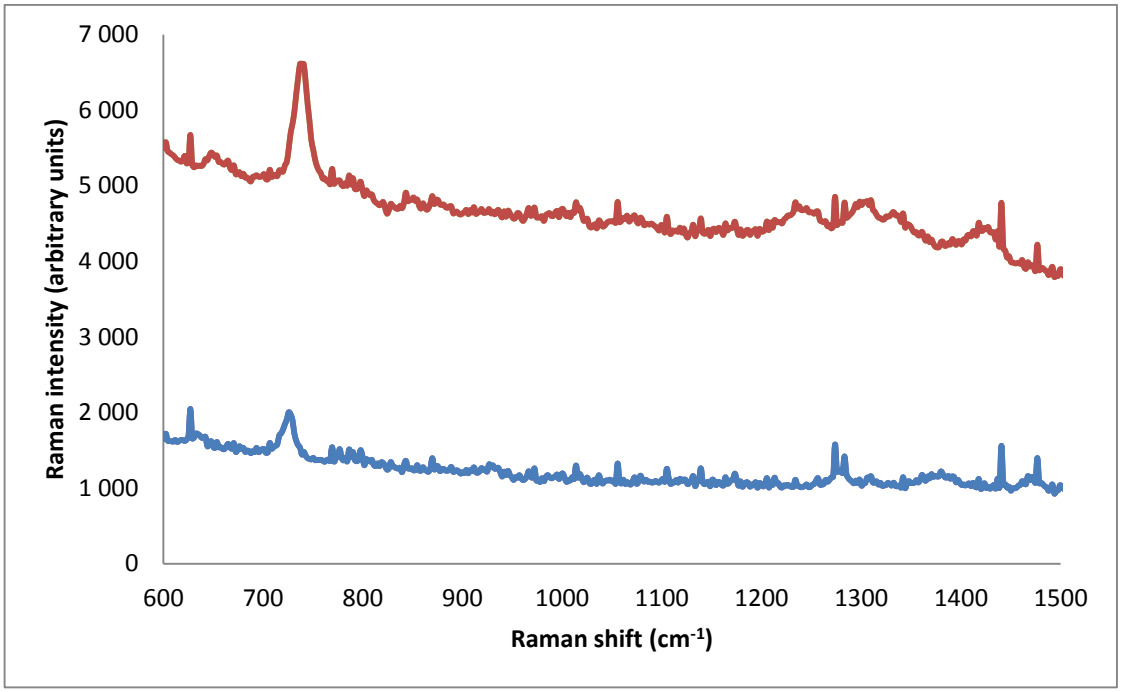

Fig. 16: Raman spectra of adenine on month old cellulose polyethylenimine coated plastic sheets with a silver layer reduced with reduction reagent glucose at concentration of 10^{-4} mol·dm^{-3} in comparison to adenine on an unmodified sheet at concentration of 10^{-1} mol·dm^{-3}

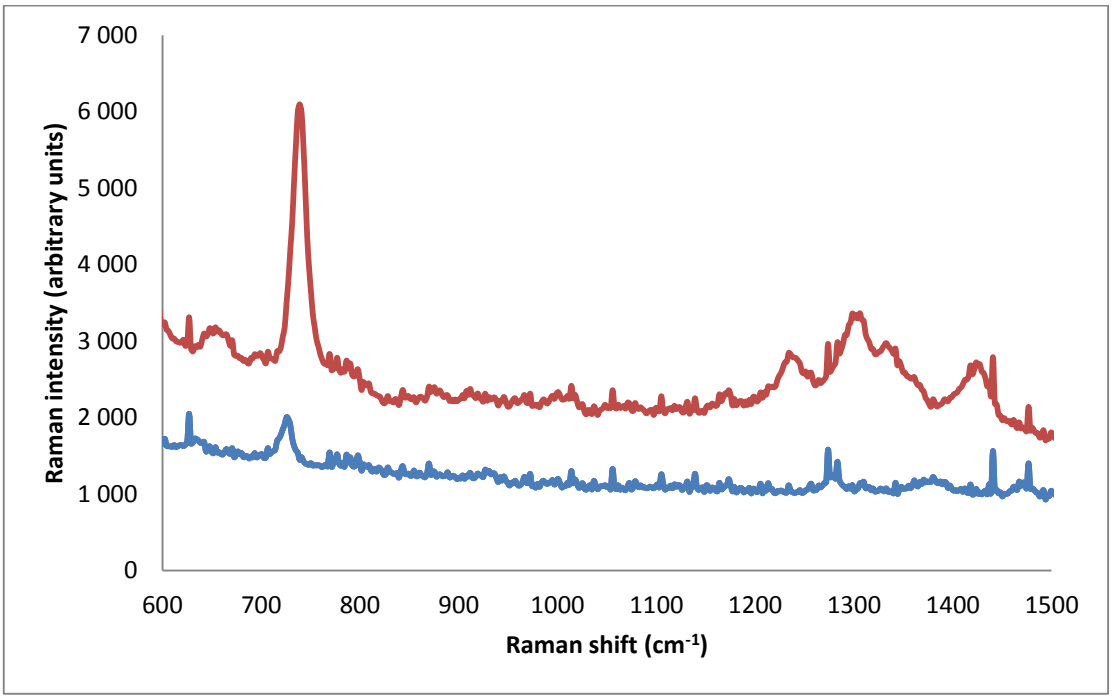

Fig. 17: Raman spectra of adenine on week old cellulose polyethylenimine coated plastic sheets with a silver layer reduced with reduction reagent glucose at concentration of 10^{-4} mol·dm^{-3} in comparison to adenine on an unmodified sheet at concentration of 10^{-1} mol·dm^{-3}

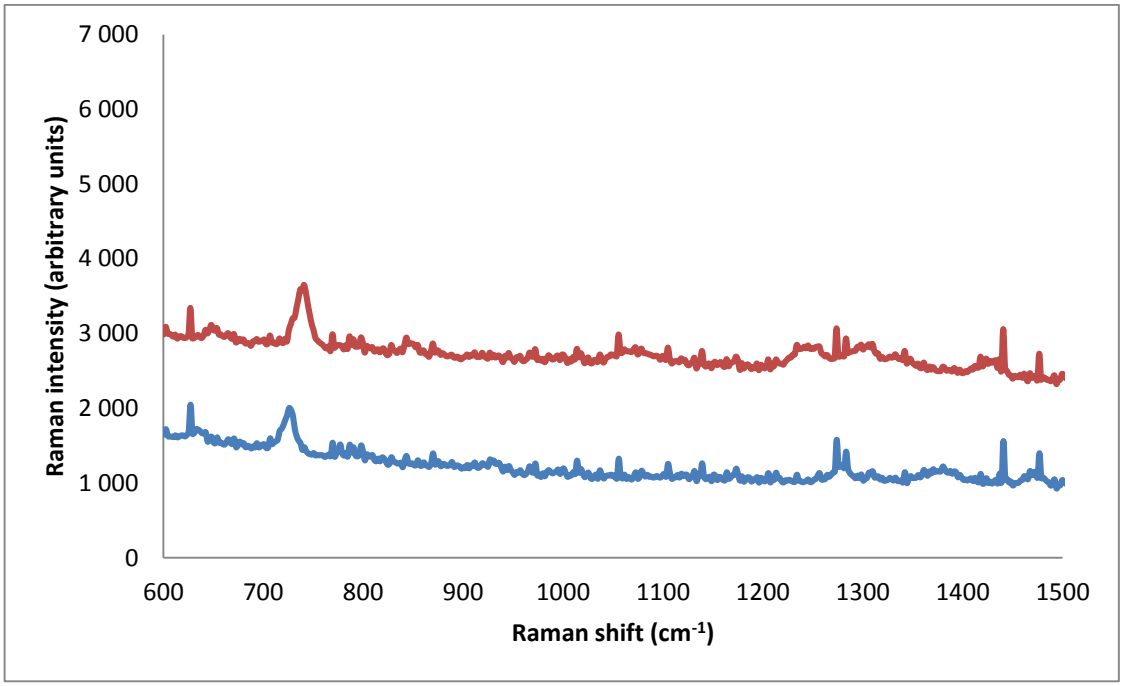

Fig. 18: Raman spectra of adenine on month old cellulose MN300 DEAE coated plastic sheets with a silver layer reduced with reduction reagent maltose at concentration of 10^{-4} mol·dm^{-3} in comparison to adenine on an unmodified sheet at concentration of 10^{-1} mol·dm^{-3}

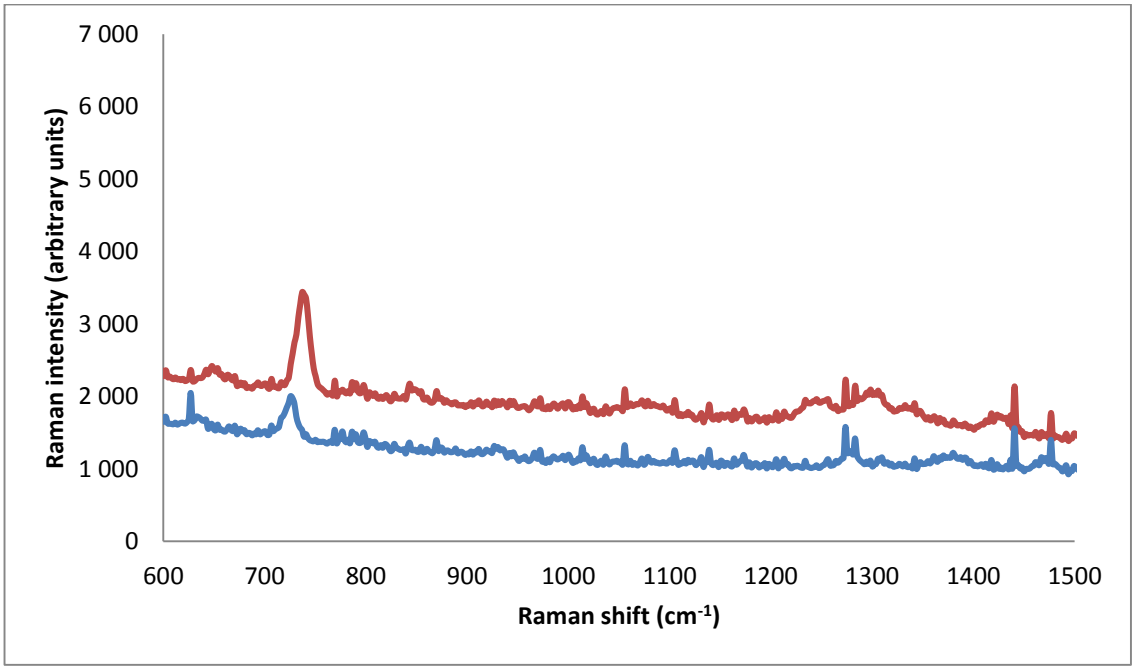

Fig. 19: Raman spectra of adenine on month old cellulose MN300 coated plastic sheets with a silver layer reduced with reduction reagent glucose at concentration of 10^{-4} mol·dm^{-3} in comparison to adenine on an unmodified sheet at concentration of 10^{-1} mol·dm^{-3}

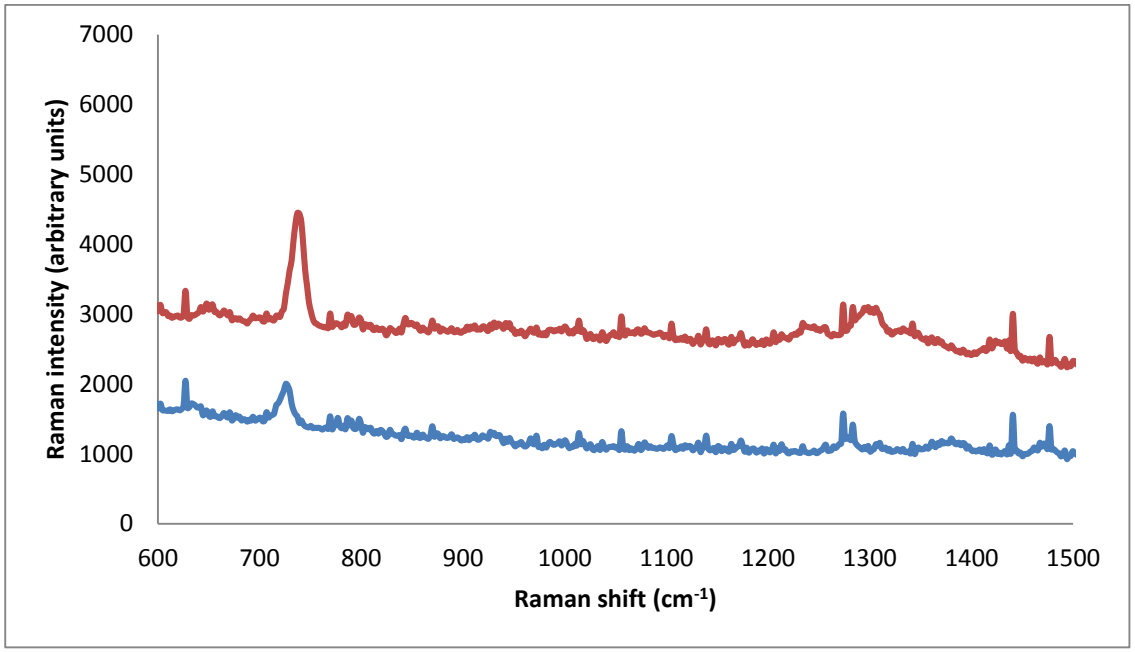

Fig. 20: Raman spectra of adenine on week old cellulose MN300 coated polyester sheets with a silver layer reduced with reduction reagent glucose at concentration of 10^{-4} mol·dm^{-3} in comparison to adenine on an unmodified sheet at concentration of 10^{-1} mol·dm^{-3}

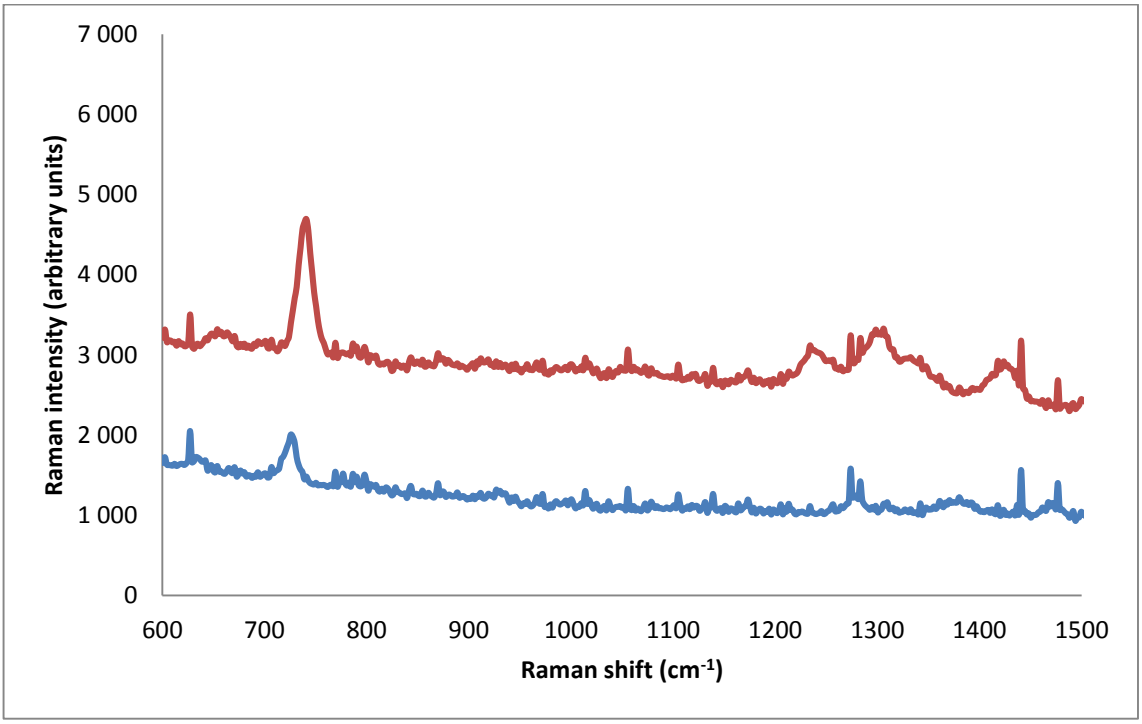

Fig. 21: Raman spectra of adenine on month old cellulose polyethylenimine coated plastic sheets with a silver layer reduced with reduction reagent maltose at concentration of 10^{-4} mol·dm^{3} in comparison to adenine on an unmodified sheet at concentration of 10^{-1} mol·dm^{-3}

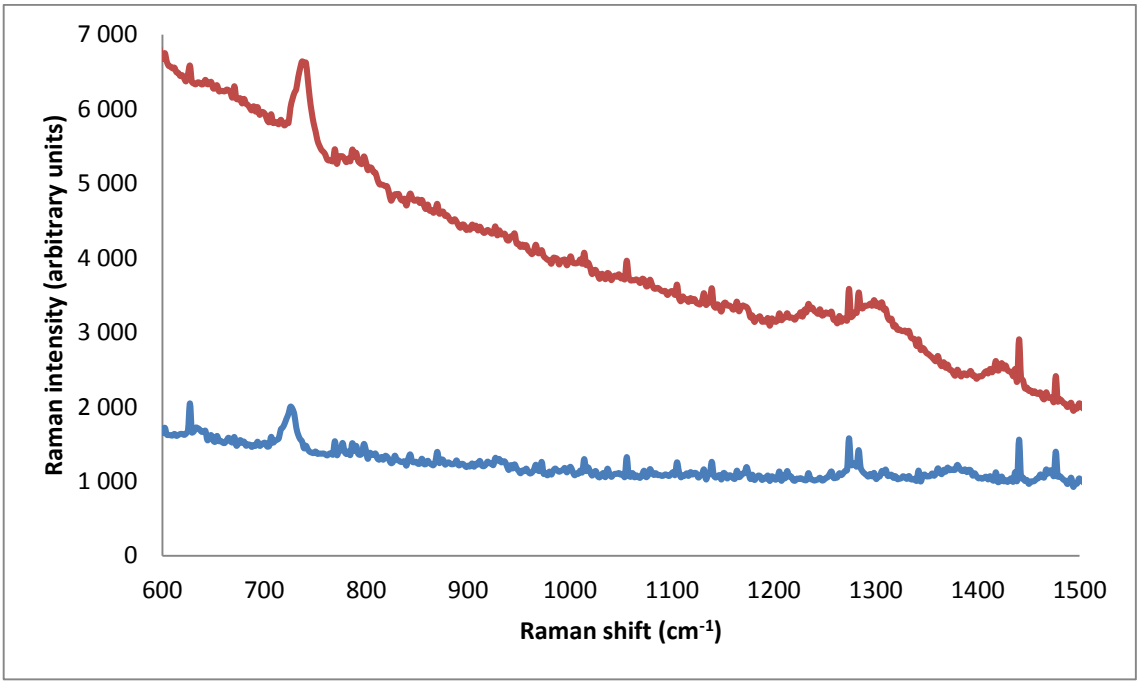

Fig. 22: Raman spectra of adenine on month old aluminium oxide N coated plastic sheets with a silver layer reduced with reduction reagent glucose at concentration of 10^{-4} mol·dm^{-3} in comparison to adenine on an unmodified sheet at concentration of 10^{-1} mol·dm^{-3}

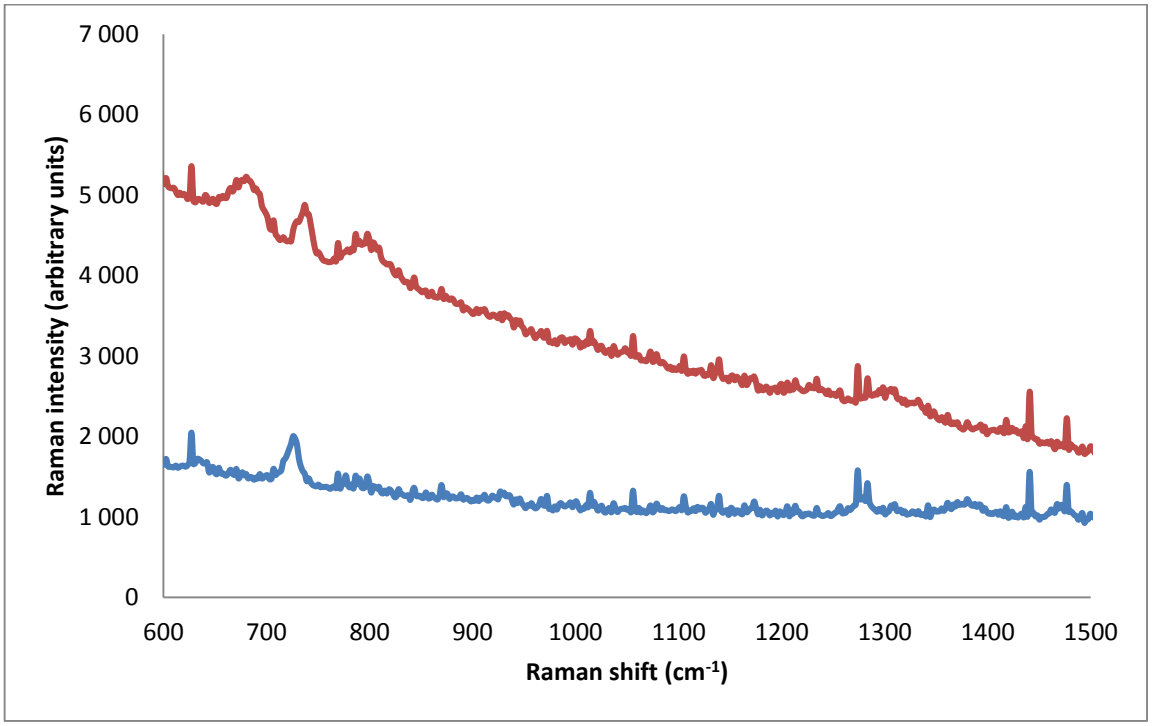

Fig. 23: Raman spectra of adenine on month old aluminium oxide N coated plastic sheets with a silver layer reduced with reduction reagent maltose at concentration of 10^{-4} mol·dm^{-3} in comparison to adenine on an unmodified sheet at concentration of 10^{-1} mol·dm^{-3}

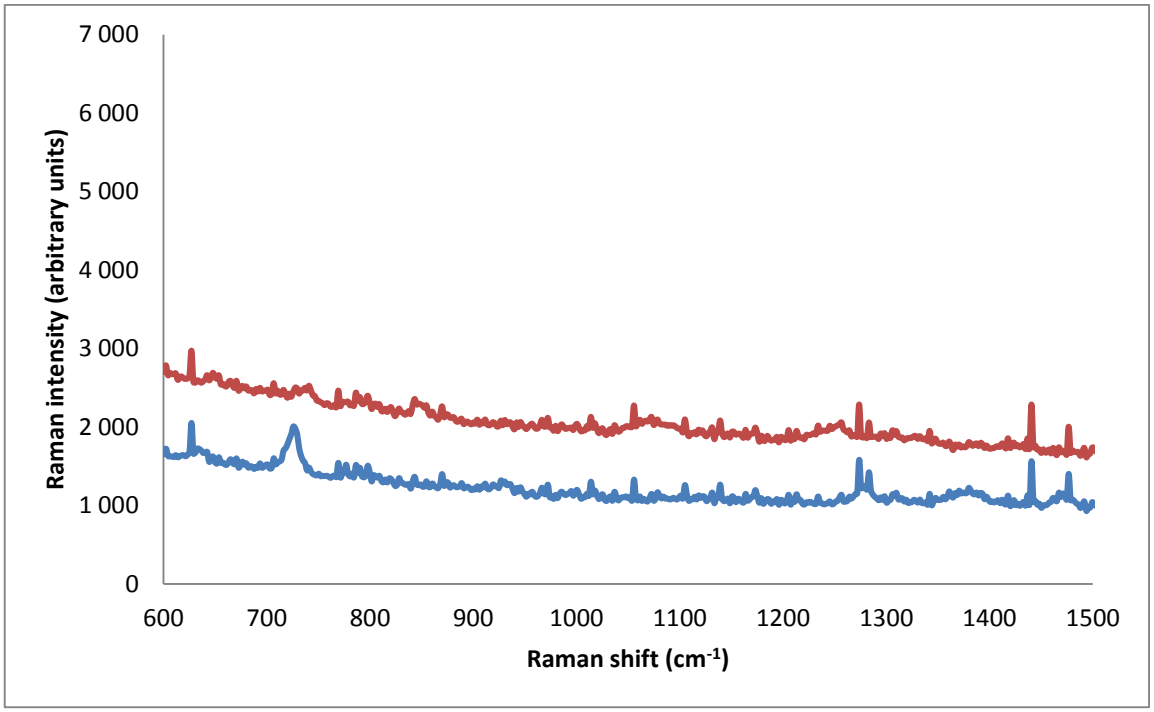

Fig. 24: Raman spectra of adenine on month old microcrystalline cellulose coated plastic sheets with a silver layer reduced with reduction reagent maltose at concentration of 10^{-4} mol·dm^{-3} in comparison to adenine on an unmodified sheet at concentration of 10^{-1} mol·dm^{-3}

Peaks for adenine showed up at 734 cm^{-1}. The peak for adenine on all of the silver coated substrates was slightly shifted, but that was due to the modification of the surface. The substrates, which were a week old, had much higher peaks than the peaks of month old substrates. When we compare Fig. 16 to Fig. 17 and Fig. 19 to Fig. 20, the peaks for adenine are much bigger in the case of the week old substrates. Therefore, strength of the peaks decreases with time. Aluminium oxide N substrates (Fig. 22, 23) did show the 734 cm^{-1} peak, but in comparison to the other substrates, the peaks weren't as strong or as sharp. With the microcrystalline cellulose substrate (Fig. 24), we can see that it didn't show any peak for adenine.

Reproducibility was proven with cellulose polyethylenimine and cellulose MN300 substrates (Fig. 16, 17 and Fig. 19, 20). Cellulose polyethylenimine sheets overall showed the best peaks with both reduction reagents, cellulose MN300 using glucose and cellulose MN300 DEAE using maltose also had very good results.

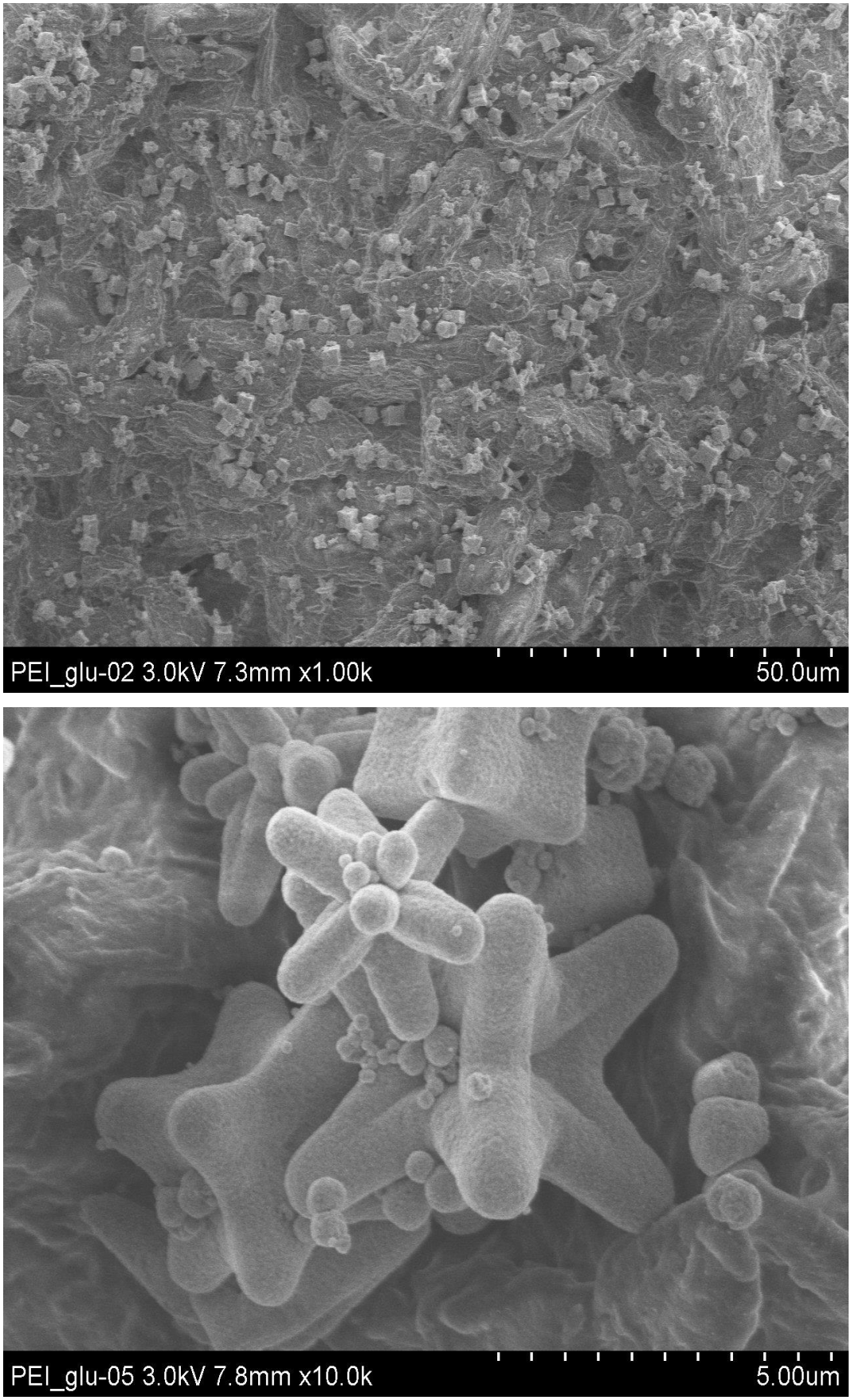

Fig. 25: SEM images of silver particle layers on a cellulose polyethylenimine substrate prepared by using glucose as a reduction reagent

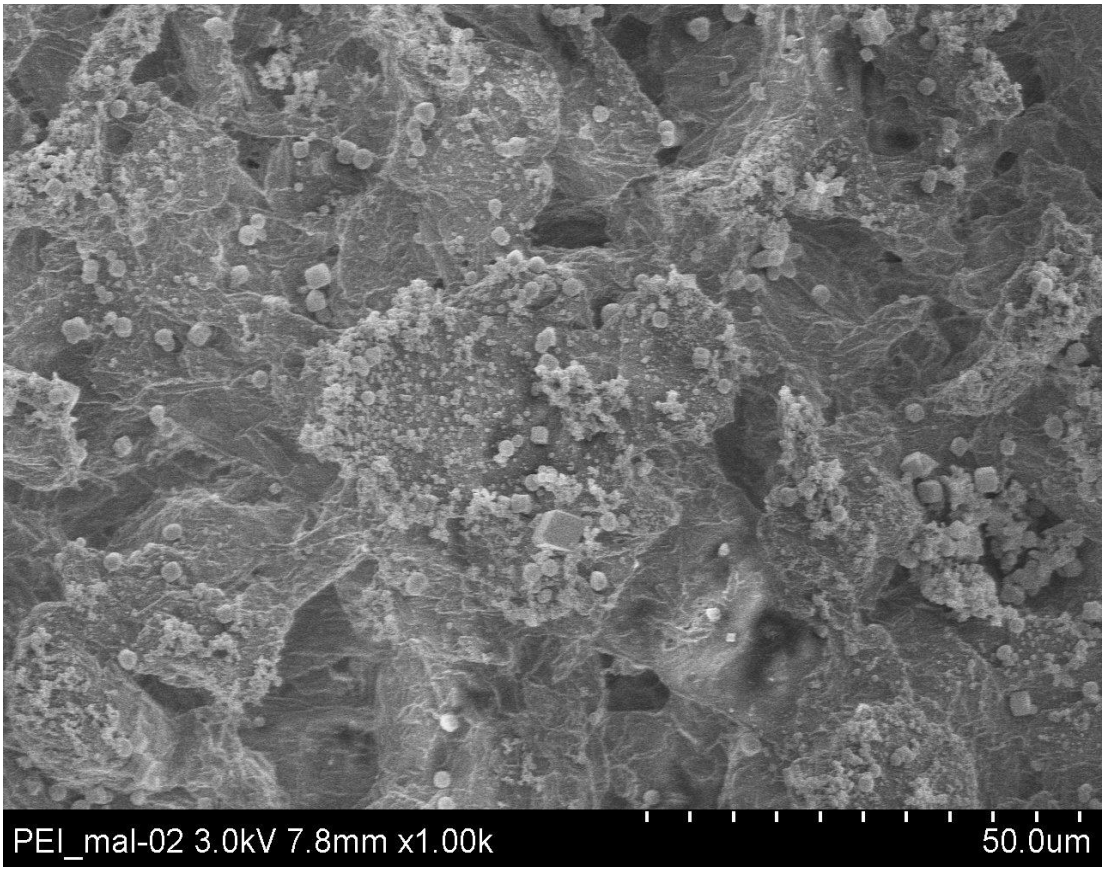

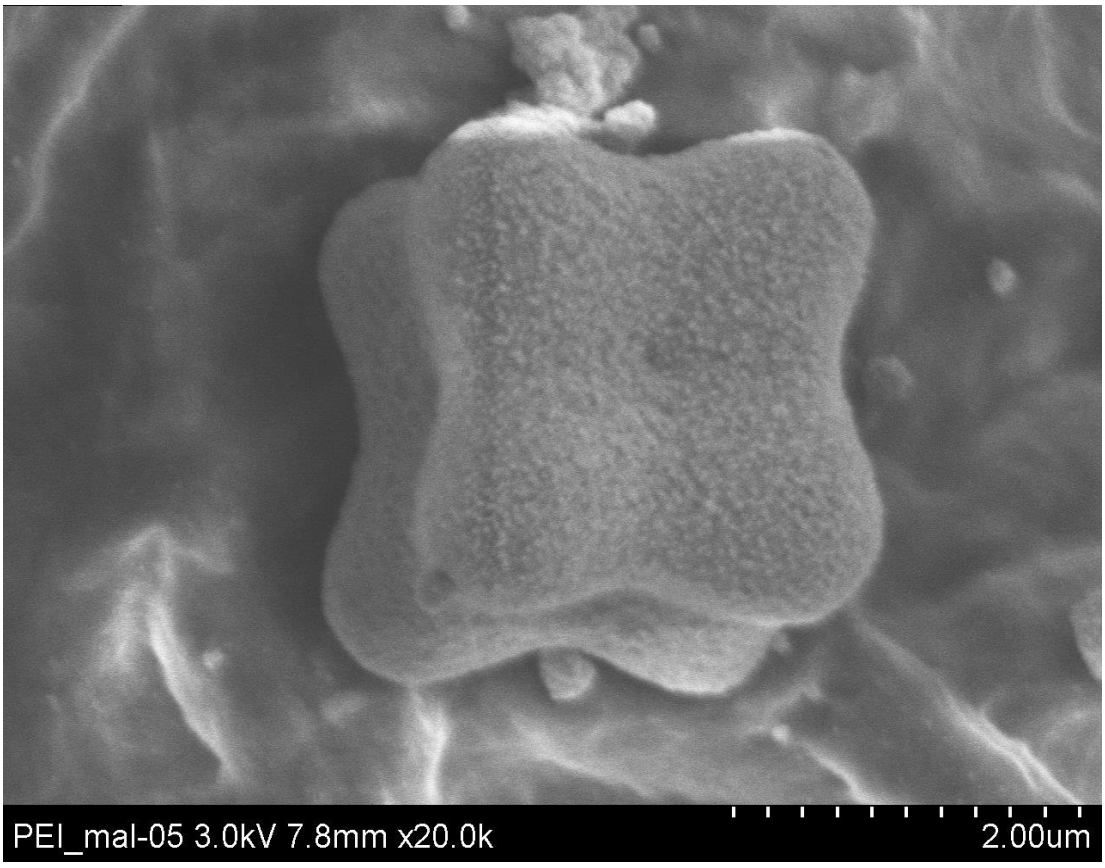

Fig. 26: SEM images of silver particle layers on a cellulose polyethylenimine substrate prepared by using maltose as a reduction reagent

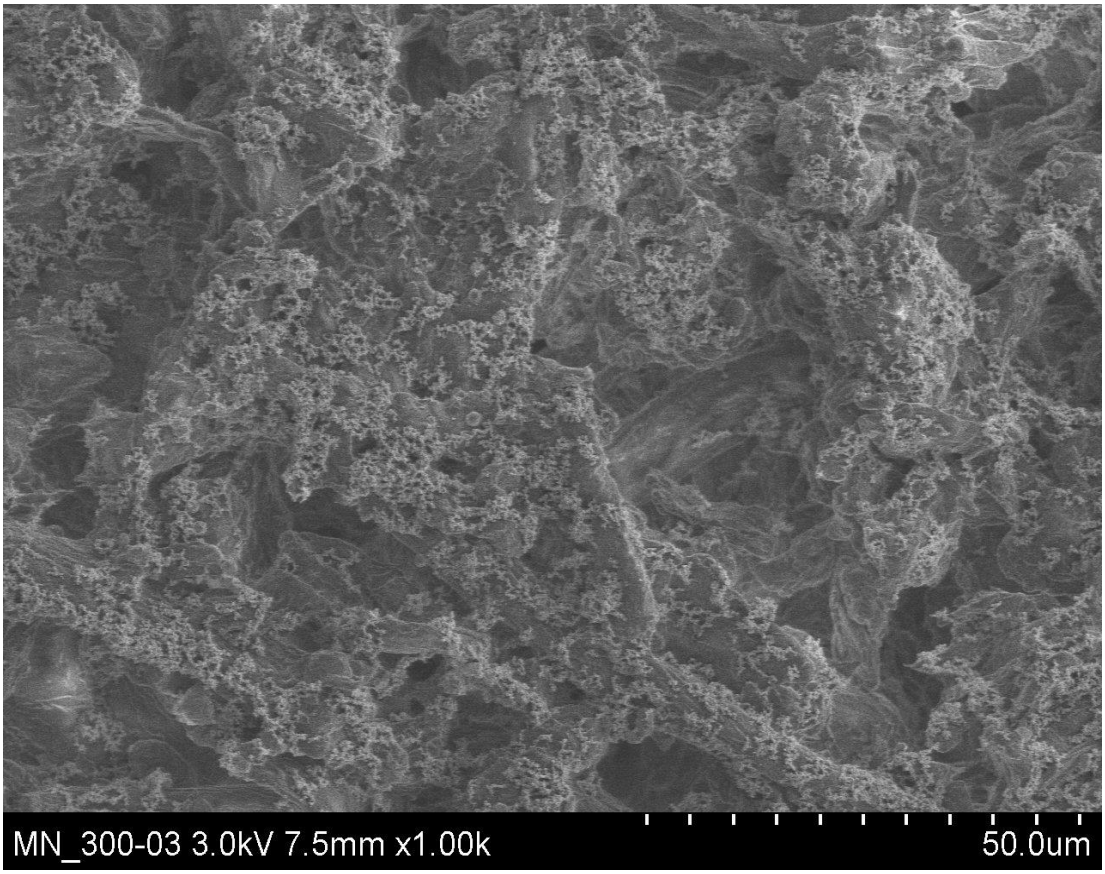

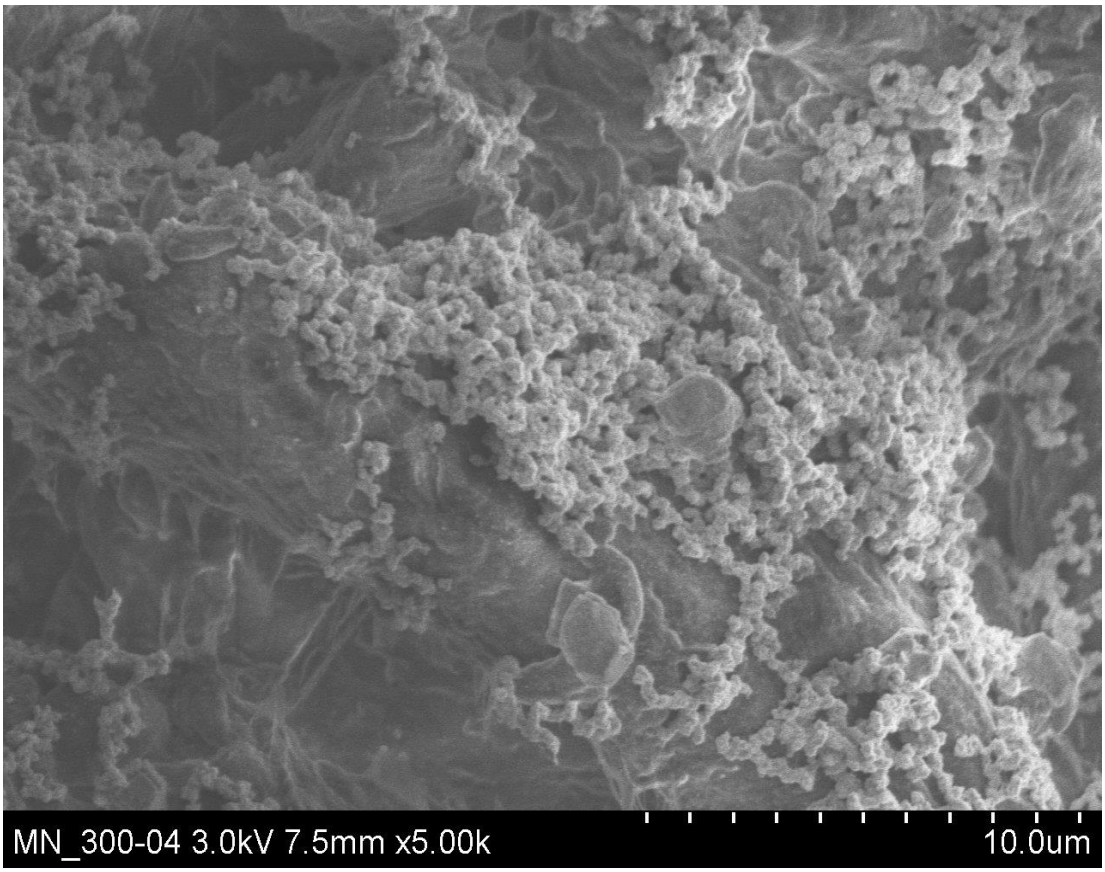

Fig. 27: SEM images of silver particle layers on a cellulose MN 300 DEAE substrate prepared by using maltose as a reduction reagent

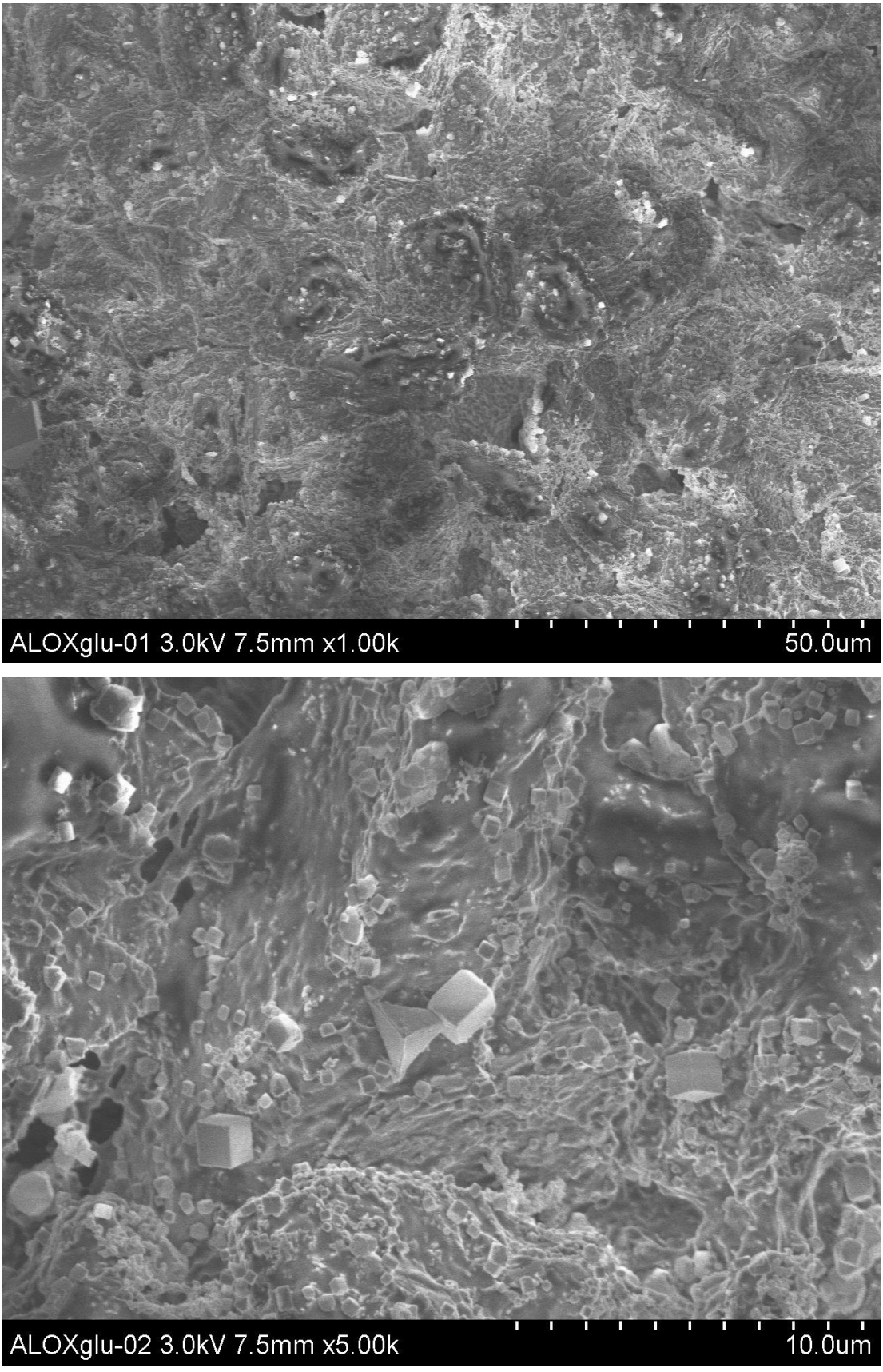

Fig. 28: SEM images of silver particle layers on an aluminium oxide N substrate prepared by using glucose as a reduction reagent

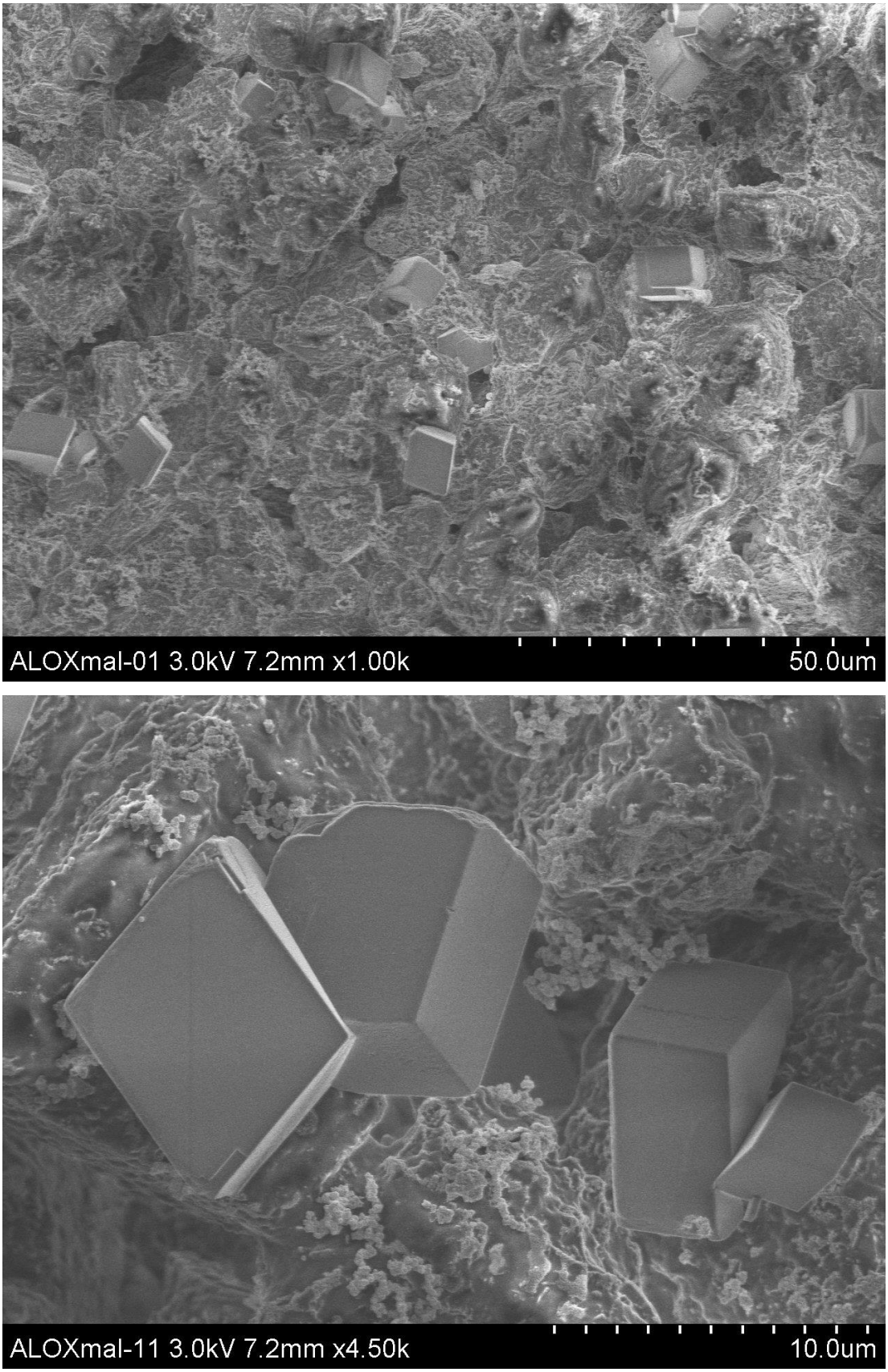

Fig. 29: SEM images of silver particle layers on an aluminium oxide N substrate prepared by using maltose as a reduction reagent

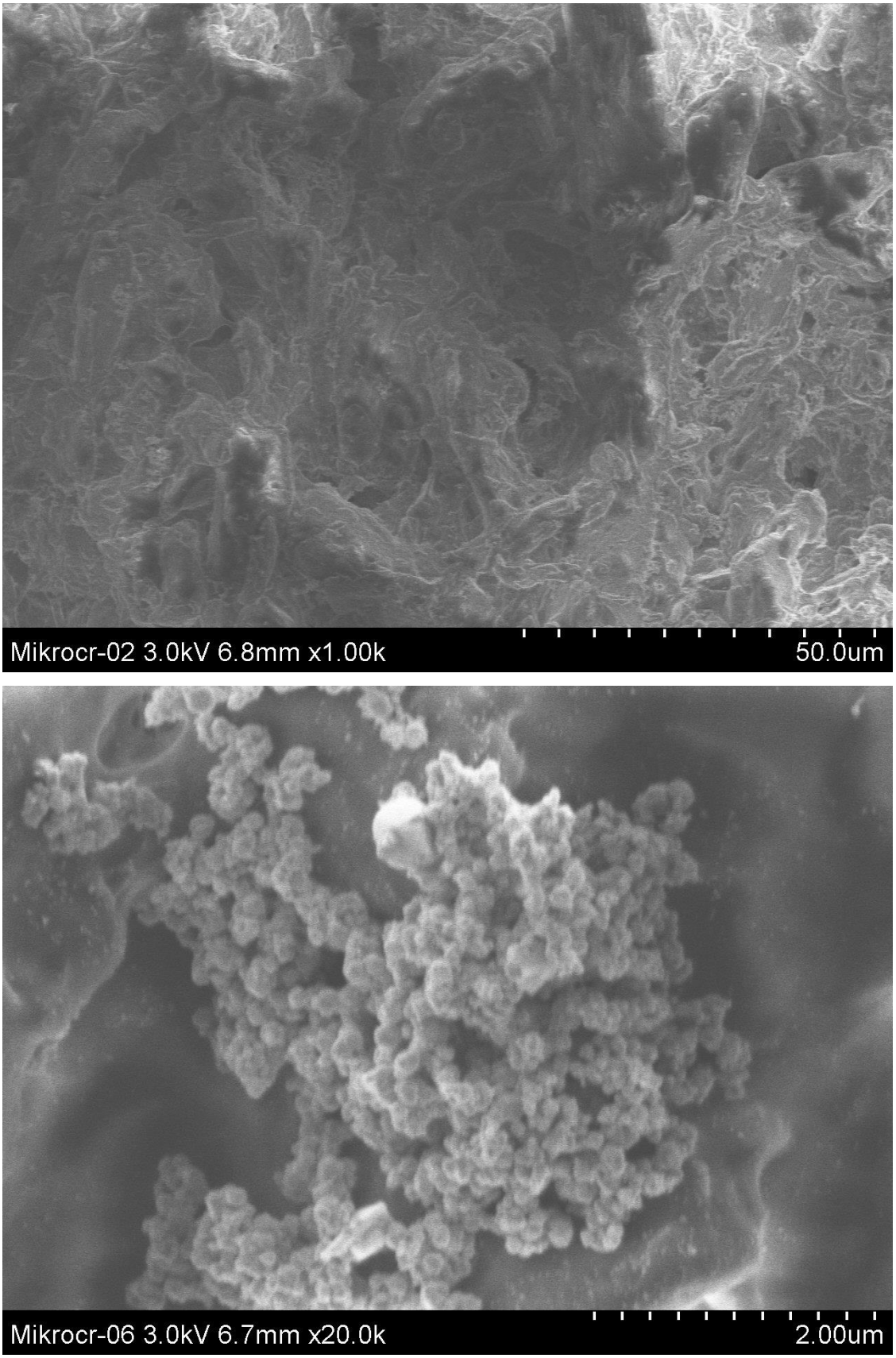

Fig. 30: SEM images of silver particle layers on a microcrystalline cellulose substrate prepared by using maltose as a reduction reagent

If we examine SEM images of the individual substrates, we can see why cellulose polyethylenimine worked the best. Silver particles were evenly dispersed on the surface of the sheets and had a very specific shape. When we used maltose as a reduction reagent, the silver particles had a shape of a cube (Fig. 26), whereas glucose reduced nanoparticles had a more complex shape, resembling a star (Fig. 25). The fact that maltose reduced sheets had a weaker signal was probably due to the shape of the nanoparticles which had a smaller adsorption surface and also because they weren't as evenly dispersed as the glucose reduced nanoparticles. In some places, we can see that they formed clusters.

Silver particles on cellulose MN300 DEAE sheets didn't have any specific shapes; they only formed clusters on the surface of the sheet (Fig. 27). They were relatively evenly dispersed which contributed to visible spectra of adenine, but compared to cellulose polyethylenimine substrates, the peak wasn't as strong. If we look at the SEM images of aluminium oxide sheets (Fig. 28, 29), we can see that there aren't as many particles dispersed on the surface. They are cube shaped which might be why we at least registered a peak for adenine, but in the case of microcrystalline cellulose (Fig. 30), there are very few nanoparticles which also do not have any specific shape. These findings again prove that the shape, size and distribution of silver nanoparticles are important characteristics for strong SERS spectra.

It can be concluded that the cellulose polyethylenimine sheets prepared with glucose as the reduction reagent showed the best results. The surface enhancement of the week old substrate was approximately $6 \cdot 10^3$.

5. Summary

The aim of this bachelor thesis was the preparation of silver particle layers for the purposes of Surface enhanced Raman spectroscopy.

Silver particle layers were prepared with a modified Tollens method. Glucose, maltose, ascorbic acid, hydroxylamine and hydrazine were tested as reduction reagents. Glucose and maltose were the most efficient, the rest could not be used due to a formation of excess clusters of silver particles. All sheets except for polyamide 6 were successfully synthesized. After synthesis, the surface enhancement of each substrate was observed at an excitation of 785 nm. This excitation wavelength was chosen because it works best with biological samples and does not cause interferences from fluorescence. Surface enhancement was measured on month old and week old substrates to compare how much the substrates deteriorate over time and showed that the adenine peaks decreased. Only the following substrates showed good Raman enhancement: cellulose polyethylenimine with glucose and maltose as reduction reagents, cellulose MN300 with glucose as a reduction reagent and cellulose MN300 DEAE with maltose as a reduction reagent. Raman surface enhancement of cellulose polyethylenimine with glucose was approximately $6 \cdot 10^3$. SEM images of these substrates demonstrated a uniform distribution of silver particles. Cellulose polyethylenimine with glucose had star shaped silver particles evenly dispersed on the surface, cellulose polyethylenimine with maltose has particles in the shape of blocks forming clusters in certain places. Aluminium oxide substrates formed cube and triangular shaped particles and cellulose MN300 DEAE and microcrystalline cellulose had big clusters of silver particles.

These substrates were prepared using a simple method giving a possibility of future mass production. It was proven, that the shape, distribution and size of silver particles all play an important role in surface enhancement. The age of substrates is also a significant factor, which can be controlled by preserving the substrates in suitable conditions. The SERS spectra were reproducible and reliable.

6. Závěr

Cílem této bakalářské práce byla příprava vrstev stříbra částic za účelem povrchově zesílené Ramanovy spektroskopie.

Stříbrné vrstvy částic byly připraveny modifikovanou Tollensovou metodou. Glukóza, maltóza, kyselina askorbová, hydroxylamin a hydrazin byly použity jako redukční činidla, avšak dále se pracovalo pouze s maltózou a glukózou, jelikož ostatní činidla při syntéze tvořily nadbytek stříbrných částic, které se nenanesly na povrch substrátů. Všechny vrstvy byly úspěšně syntetizované kromě polyamidu 6. Po syntéze bylo pozorováno povrchové zesílení každého substrátu při excitační vlnové délce 785 nm. Tato vlnová délka byla vybrána, jelikož je nejlépe využitelná pro detekci biologických vzorků, kdy fluorescence nezpůsobuje tolik interferencí. Povrchové zesílení bylo změřené na substrátech, které byly měsíc a týden staré, aby se daly porovnat změny v signálech a ukázaly, že signál adeninu slábne s časem. Pouze tyto substráty vykazovaly dobré Ramanovo zesílení: celulóza polyethylenimin s glukózou a maltózou jako redukční činidla, celulóza MN300 s glukózou jako redukční činidlo a celulóza MN300 DEAE s maltózou jako redukční činidlo. Ramanovo povrchové zesílení celulózy polyethylenimin substrátu s glukózou bylo zhruba $6 \cdot 10^3$. SEM snímky těchto substrátů ukázaly rovnoměrné rozmístění stříbrných částic na jejich povrchu. Celulóza polyethylenimin s glukózou měl pravidelně rozmístěné hvězdicovité stříbrné částice na povrchu, celulóza polyethylenimin s maltoźou vytvořil kvádrové částice, které se místy shlukovaly. Substráty oxidu hlinitého vytvářely částice ve tvaru krychle a trojúhelníku a celulóza MN300 DEAE a mikrokrystalická celulóza měly na svém povrchu velké shluky stříbrných částic.

Tyto substráty byly připraveny jednoduchou metodou umožňující budoucí masovou výroby. Bylo prokázáno, že tvar a rozmístění nanočástic stříbra hrají důležitou roli v povrchovém zesílení. Stáří substrátů je taky velmi důležitý aspekt, který může ovlivnit uchovávání substrátů ve vhodném prostředí. SERS spektra byly reprodukovatelné a spolehlivé.

7. References

1. Fleischmann, M.; Hendra, P. J.; McQuillan, A. J.; Raman spectra of pyridine adsorbed at a silver electrode, *Chem. Phys. Lett*, 1974, 26, 163-66

2. Li, D.; Li, D.-W.; Fossey, J. S.; Long, Y.-T.; Portable Surface-Enhanced Raman Scattering Sensor for Rapid Detection of Aniline and Phenol Derivatives by On-Site Electrostatic Preconcentration, *Anal. Chem.*, 2010, 82, 9299-9305

3. Guerrini, L.; Garcia-Ramos, J. V.; Domingo, C.; Sanchez-Cortes, S.; Sensing Polycyclic Aromatic Hydrocarbons with Dithiocarbamate-Functionalized Ag Nanoparticles by Surface-Enhanced Raman Scattering, *Anal. Chem.*, 2009, 81, 953-960

4. Chen, K.; Han, H.; Luo, Z.; Streptococcus suis II immunoassay based on thorny gold nanoparticles and surface enhanced Raman scattering, *Analyst*, 2012, 137, 1259-1264

5. Xue, J.-Q.; Li, D. W.; Qu, L.-L.; Long, Y.-T.; Surface-imprinted core-shell Au nanoparticles for selective detection of bisphenol A based on surface-enhanced Raman scattering, *Analytica Chimica Acta 777*, 2013, 57-62

6. Mahmoud, K. A.; Zourob, M.; Fe_3O_4/Au nanoparticles/lignin modified microspheres as effectual surface enhanced Raman scattering (SERS) substrates for highly sensitive detection of 2,4,6-trinitrotoluene (TNT), *Analyst*, 2013, 138, 2712-2719

7. Tang, H.; Meng, G.; Huang, Q.; Zhang, Z.; Huang, Z.; Zhu, C.; Arrays of Cone-Shaped ZnO Nanorods Decorated with Ag Nanoparticles as 3D Surface-Enhanced Raman Scattering Substrates for Rapid Detection of Trace Polychlorinated Biphenyls, *Adv. Fund. Mater.*, 2012, 22, 218-224

8. Qu, L.-L.; Li, D.-W.; Xue, J.-Q.; Zhai, W.-L.; Fossey, J. S.; Long, Y.-T.; Batch fabrication of disposable screen printed SERS arrays, *Lab Chip*, 2012, 12, 876-881

9. Bantz, K. C.; Haynes, C. L.; Surface-enhanced Raman scattering detection and discrimination of polychlorinated biphenyls, *Vibrational Spectroscopy*, 2009, 50, 29-35

10. He, L.; Lin, M.; Li, H.; Kim, N.-J.; Surface-enhanced Raman spectroscopy coupled with dendritic silver nanosubstrate for detection of restricted antibiotics, *J. Raman Spectrosc.*, 2010, 41, 739-744

11. Wang, Y.; Lee, K.; Irudayaraj, J.; Silver Nanosphere SERS Probes for Sensitive Identification of Pathogens, *J. Phys. Chem. C*, 2010, 114, 16122-16128

12. He., L.; Deen, B.; Rodda, T.; Ronningen, I.; Blasius, T.; Haynes, C.; Diez-Gonzales, F.; Labuza, T. P.; Rapid Detection of Ricin in Milk Using Immunomagnetic Separation Combined with Surface-Enhanced Raman Spectroscopy, *Journal of Food Science*, 2011, 76, 5, 49-53

13. Kudo, H.; Itoh, T.; Kashiwagi, T.; Ishikawa, M.; Takeuchi, H.; Ukeda, H.; Surface enhanced Raman scattering spectroscopy of Ag nanoparticles aggregates directly photo-reduced on pathogenic bacterium (Helicobacter pylori), *Journal of Photochemistry and Photobiology A: Chemistry*, 2011, 221, 181-186

14. Fan, C.; Hu, Z.; Riley, L. K.; Purdy, G. A.; Mustapha, A.; Lin, M.; Detecting Food- and Waterborne Viruses by Surface-Enhanced Raman Spectroscopy, *Journal of Food Science*, 2010, 75, 5, 302-307

15. Driskell, J. D.; Kwarta, K. M.; Lipert, R. J.; Porter, M. D.; Low-Level Detection of Viral Pathogens by a Surface-Enhanced Raman Scattering Based Immunoassay, *Anal. Chem.*, 2005, 77, 6147-6154

16. Chon, H.; Lim, C.; Ha, S.-M.; Ahn, Y.; Lee, E. K.; Chang, S.-I.; Seong, G. H.; Choo, J.; On-Chip Immunoassay Using Surface-Enhanced Raman Scattering of Hollow Gold Nanospheres, *Anal. Chem.*, 2010, 82, 5290-5295

17. Knauer, M.; Ivleva, N. P.; Niessner, R.; Haisch, C.; A flow-through microarray cell for the online SERS detection of antibody-captured E. coli bacteria, *Anal. Bioanal. Chem.*, 2012, 402, 2663-2667

18. Qu, L.-L.; Li, D.-W.; Qin, L.-X.; Mu, J.; Fossey, J. S.; Long, Y.-T.; Selection and Sensitive Detection of Intracellular $O_2^{\cdot -}$ Using Au NPs/ Cytochrome c as SERS Nanosensors, *Anal. Chem.*, 2013, 85, 9549-9555

19. Dasary, S. S. R; Singh, A. K.; Senapati, D.; Yu, H.; Ray, P. C.; Gold Nanoparticle Based Label-Free SERS Probe for Ultrasensitive and Selective Detection of Trinitrotoluene, *J. Am. Chem. Soc.*, 2009, 131, 13806-13812

20. Xu, Z.; Hao, J.; Braida, W.; Strickland, D.; Li, F.; Meng, X.; Surface-Enhanced Raman Scattering Spectroscopy of Explosive 2,4-Dinitroanisole using Modified Silver Nanoparticles, *Langmuir*, 2011, 27, 13773-13779

21. Raman, C. V.; Krishnan, K. S.; A new type of secondary radiation, *Nature*, 1921, 121, 501-502

22. Smith, E.; Dent, G.; *Modern Raman Spectroscopy – A Practical Approach*, 1.edition, Wiley, 2005, ISBN: 978-0471497943

23. http://www.doitpoms.ac.uk/tlplib/raman/printall.php (downloaded on: 2. 4. 2015)

24. Le Ru, E. C.; Etchegoin, P. G.; *Principles of Surface-Enhanced Raman Spectroscopy and related plasmonic effects,* 1.edition, Elsevier Science, 2008, ISBN: 978-0444527790

25. Moskovits, M.; Surface enhanced Raman spectroscopy: a brief retrospective, *J. Raman Spectrosc.,* 2005, 36, 485-496

26. http://hyperphysics.phy-astr.gsu.edu/hbase/atmos/imgatm/mie.gif (downloaded on 2. 4. 2015)

27. Kvítek, L.; Panáček, A.; *Základy koloidní chemie*, 1. edition, Olomouc: Univerzita Palackého v Olomouci, 2007, ISBN: 978-80-244-1669-4

28. Jensen, T.; Kelly, L.; Lazarides, A.; Schatz, G. C.; Electrodynamics of Noble Metal Nanoparticles and Nanoparticle Clusters, *Journal of Cluster Science,* 10, 2, 1999

29. Kinnan, M. K.; Chumanov, G.; Plasmon Coupling in Two-Dimensional Arrays of Silver Nanoparticles: II. Effect of the Particle Size and Interparticle Distance, *J. Phys. Chem. C,* 2010, 114, 7496-7501

30. Hao, E.; Schatz, G. C.; Hupp, J. T.; Synthesis and Optical Properties of Anisotropic Metal Nanoparticles, *Journal of Fluorescence*, 2004, 14, 4, 331-341

31. Lin, X.-M.; Cui, Y.; Xu, Y.-H.; Ren, B.; Tian, Z.-Q.; Surface-enhanced Raman spectroscopy: substrate-related issues, *Anal Bioanal Chem*, 2009, 394, 1729–1745

32. "Polychlorinated Biphenyls (PCBs): Basic information", U.S. Environmental Protection Agency, 2013 <http://www.epa.gov/epawaste/hazard/tsd/pcbs/about.htm>

33. Jarvis, R. M.; Goodacre, R.; Characterisation and identification of bacteria using SERS, *Chem. Soc. Rev.*, 2008, 37, 931-936